Field Guide Day 2 - Redwood Creek Basin

By Harvey Kelsey, Department of Geology, Western Washington University, Bellingham, WA; Mary Savina, Department of Geology, Carleton College, Northfield, MN; Iverson, R. M., U.S.G.S. David A. Johnston Cascades Volcano Observatory, Vancouver, Washington; Sonnevil, Ron, Redwood National Park, Orick, CA; LaHusen, Richard, Redwood National Park, Orick, CA, Popenoe, James, Redwood National Park, Orick, CA; Ricks, Cynthia, Siskiyou National Forest, Gold Beach, OR; and Madej, Mary Ann, Redwood National Park, Arcata, CA.

The Redwood Creek basin is underlain by somewhat different rock types from those we saw yesterday in the Van Duzen basin. The geomorphic processes, however, are comparable. In addition, the Redwood Creek basin has been studied in depth since the establishment and subsequent expansion of Redwood National Park in 1968 and 1978. The park now occupies the lower third of the basin. The extensive work of Janda and others (1975) provided the background for many of the more recent studies that will be discussed today. Among the many geomorphic studies in Redwood Creek, recent studies by Iverson (1984), Sonnevil and others (this volume), LaHusen (this volume) and others have concentrated on the detailed mechanics of landslide movement, including the relation between movement rates and styles and ground water. Both the technical aspects of these studies (including the instrumentation designs and placement of piezometers and movement monitors) and the geologic implications of the results are of great interest, and can be applied to similar types of landslides in other parts of the north coastal area.

Redwood Creek basin has also been the site of detailed sediment budget and sediment storage measurements (Madej, 1984). We will see Redwood Creek at two places: one at mid-basin in Redwood Valley near the confluence of Minor Creek (a major tributary) and one at the estuary of Redwood Creek near the town of Orick (see Fig. 21 for locations). Madej will discuss the results of her sediment budget studies at the lunch stop at Redwood Creek estuary.

One of the main reasons for concern and interest in the geomorphic processes of Redwood Creek basin is the potential for disruption of the natural environment within the national park, which originally included only the old-growth forests near the downstream end of Redwood Creek. The park was expanded in 1978 to include parts of the basin upslope of the initial park boundaries. The upper two-thirds of the Redwood Creek basin, including the area we will see from Stop 1, are still in private hands. Treatment of the newly-acquired park lands, most of which were logged and had roads built on them in the 1950s, 1960s, and early to mid-1970s, is a continuing source of concern to the Park Service. In recent storms, for instance, many road fills failed in debris flows. Debris torrents moving downstream from these flows entered the old-growth areas of the park. Redwood National Park has embarked on a process of rehabilitation of the formerly logged areas, in order to protect the natural environment of the old-growth forests. Most of the rehabilitation

is concentrated on the removal of the logging road system in that portion of the park acquired in 1978. For those interested, Redwood National Park geologists will lead an informal field trip through some of the rehabilitation sites on June 22. Today, we will be shown some of the research aimed at determining what rehabilitation measures will be the most effective in preventing slope failures from previously-logged areas. This research is also leading to a better understanding of landslide processes, soil genesis, and groundwater movement in the Redwood Creek basin.

Road Log:

We plan to leave the campground at 7:30 a.m. An early, prompt start is necessary because of the amount of driving between stop 1 and Orick.

Mileage:

0.0 Highway 299 East on-ramp near West End Road. For the first 16 miles of the trip, Highway 299 runs in the north part of the Mad River Basin.

10.2 Bridge over North Fork of Mad River.

16.4 Lord Ellis Summit, 2262 ft., the divide between Mad River basin and Redwood Creek basin. Mr. Lord and Mr. Ellis were two gentlemen around the turn of the century who were instrumental in having this road built. At about the summit, the road crosses the Bald Mountain Fault, separating Franciscan melange on the southwest from Redwood Creek schist on the northeast. The southwest side of the Redwood Creek basin is formed on the Redwood Creek schist. Through much of its length, Redwood Creek parallels the Grogan Fault, which separates schists on the southwest from Franciscan Assemblage rocks on the northeast which in this area are sandstones and mudstones (see Fig. 22).

17.4 Junction Redwood Valley Road. Take a left onto Redwood Valley Road. (Highway 299 continues east into the Trinity River basin and on to the Central Valley.) We are now travelling northeast into the axis of the Redwood Creek valley.

17.65 View ahead across the Redwood Creek basin to the Minor Creek drainage and Minor Creek earthflow.

18.4 Roadcuts on the left expose the Redwood Creek schist. The schist is similar in lithology and metamorphic grade to the South Fork Mountain Schist which is the easternmost unit of the Franciscan Assemblage in much of the northern Coast Ranges. The Redwood Creek schist may be a sliver from South Fork Mountain, moved northwest along the Grogan fault (Kelsey and Hagans, 1982).

When we worked on the road log for this part of the trip in August, 1984, Redwood Valley Road, a major county road, was in terrible shape. Slope failures had removed the entire northbound lane in some places, and tension cracks and bumps were ubiquitous. While we hope that the road

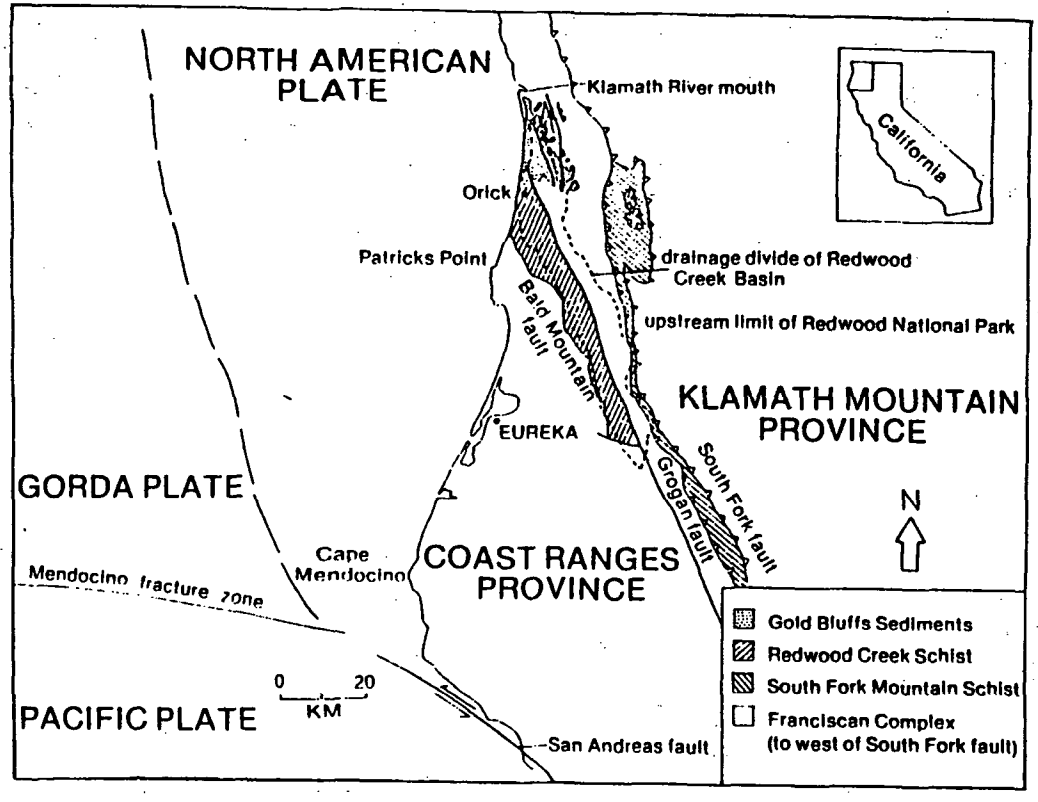

Figure 22. Generalized geologic and tectonic map of north coastal California showing major faults and rock units in the Redwood Creek drainage basin. Note that the Grogan fault separates Redwood Creek schist from Franciscan Assemblage sandstones and mudstones. From Kelsey, in press.

will be open for us on this trip, we also hope that some of the evidence of the stability problems in the Redwood Creek schist remains for you to see. This afternoon, we will have a detailed look at the soils formed on the Redwood Creek schist and the stability problems posed by those soils, which are the subject of Rick LaHusen's thesis.

20.0 View ahead to Minor Creek earthflow, our first stop.

20.8 Bridge over Redwood Creek. The bridge is near the upstream end of Redwood Valley, a mile-long alluvial valley in the middle of the Redwood Creek basin. This low-gradient, wide-channel reach separates steep-gradient, narrow reaches upstream and downstream which have a well-developed inner gorge morphology. Kelsey (in press) has proposed that the head of Redwood Valley marks the downstream end of a reach of Redwood Creek where the creek is capable of moving sediment down channel. In Redwood Valley, the channel gradient has decreased to the point where the stream can no longer transport sediment, so it has been deposited, forming the wider valley. With a reduced sediment load, Redwood Creek begins to re-incise at the downstream end of Redwood Valley, creating a second reach with inner gorge slopes (see Fig. 23).

21.25 Junction with Hoopa Road, take right. Road in this section crosses the Grogan Fault Zone within a few hundred meters of the road junction. Note the change from schist to sandstone in the road cuts.

21.7 Outcrops of sandstone indicate that road is now east of the Grogan Fault.

22.05 Chert block on right.

22.3 Road begins to traverse Minor Creek earthflow.

STOP 1 - MINOR CREEK LANDSLIDE
Park here along the north (left) side of the road and walk about 150 m upslope along the west edge of the earthflow. We will immediately convene near the upper west edge of the earthflow for a brief lecture. We will then have about 1 1/2 hours to examine the earthflow and its instrumentation.

MINOR CREEK LANDSLIDE, By R. M. Iverson

Minor Creek landslide has been monitored by the U.S. Geological Survey for the past 13 years. As part of a broad-based study of the effects of upstream sediment sources on the behavior of Redwood Creek, transverse stake lines and rain gages were installed on Minor Creek landslide and several nearby landslides in the early 1970s (e.g. Harden, et. al., 1978). During the late 1970s and early 1980s, more instrumentation was added to the monitoring network at Minor Creek landslide. This instrumentation included two flumes in which water and sediment discharges of axial gullies were measured; 15 inclinometer tubes in which subsurface deformation was measured, two continuously recording surface extensometers or "strain

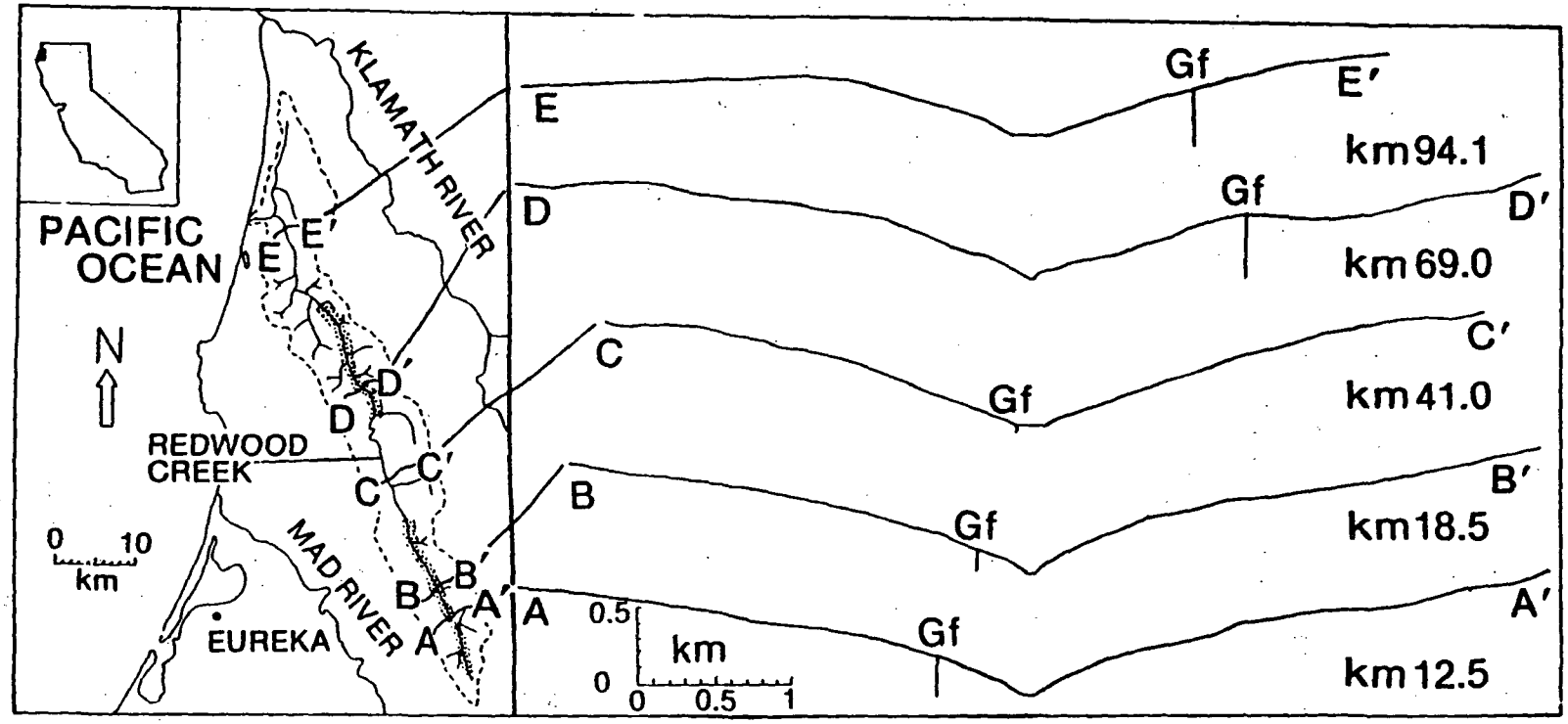

Figure 23. Topographic profiles, perpendicular to the course of Redwood Creek, drawn along interfluves between tributary basins. For each profile, the two halves represent the nearest opposing interfluves, which are offset along the creek by no more than 500 m. Map of Redwood Creek basin shows locations of the topographic profiles and the two mainstem channel reaches (stippled areas) where an inner gorge is moderately to well developed. Gf: location of Grogan fault on profile, sandstone and mudstone to east of fault and schist to west of fault. From Kelsey, in press.

gages"; 64 open standpipe piezometers; three electrical piezometers, one of which was fitted with a continuous recorder; and a longitudinal stake line that incorporated several strain rhombs. Most of this instrumentation is still in service. The density and longevity of the data collection network at Minor Creek landslide make it nearly unique among landslides that have not been modified by extensive geotechnical engineering.

The current data collection network and morphology of Minor Creek landslide are depicted on maps shown here as Figures 24, 25, and 26. These maps provide a good basis for a self-guided tour of the landslide. So that you may easily locate the mapped features, several key areas will be marked in the field. These include the west ends of the five transverse stake lines, the recording extensometer, several inclinometer tubes, and the recording electrical piezometer. Morphological features you should be certain to examine include the highly disrupted landslide toe and the discontinuous "mole tracks" of dilated soil along the landslide's lateral shear zones.

Conspicuous on the landslide surface are many stakes and standpipes. Orange stakes are members of transverse stake lines and red stakes are longitudinal-line or strain-rhomb stakes. Stakes of other colors are also present but are no longer monitored. Small-diameter, white plastic pipes are open piezometers with casing perforated at specific depths. The pipes are numbered on the outside and the perforation depths are generally written inside the pipe caps. Large-diameter, white plastic pipes contain electrical piezometer leads and air ports and green pipes and aluminum pipes are inclinometer access tubes. Most of these pipes contain water all year long. Many of the pipes have been sheared off or constricted where they pass through the base of the landslide.

The status of Minor Creek landslide data collection and analysis through June 1984 has been summarized by Iverson (1984). Several reports in press or in review as of January 1985 describe interpretation of the data and theoretical work that has been motivated by the data (Iverson, 1985 a, b, c, d, e; Nolan and Janda, 1985). Salient aspects of the data are summarized in Figures 27 through 33 shown here.

Figure 27 depicts rainfall, piezometric response, and landslide displacement data recorded at the extensometer site during two annual landslide movement cycles. These data are representative of most movement cycles and they provide many insights to the behavior of Minor Creek landslide. Particularly interesting are the remarkably steady landslide movements that follow brief annual periods of acceleration. Acceleration is motivated by gradual changes in ground-water seepage, pore pressure, and effective stress that occur during the onset of the rainy season, whereas steady motion occurs in response to a temporally steady stress state and reflects a dynamic balance between driving and resisting forces. This dynamic force balance is suggestive of a viscous component of deformation resistance, which holds major implications for understanding long-term landslide behavior.

Subsurface deformation of Minor Creek landslide has been monitored by repetitive inclinometer surveys of bore-hole casing displacement.

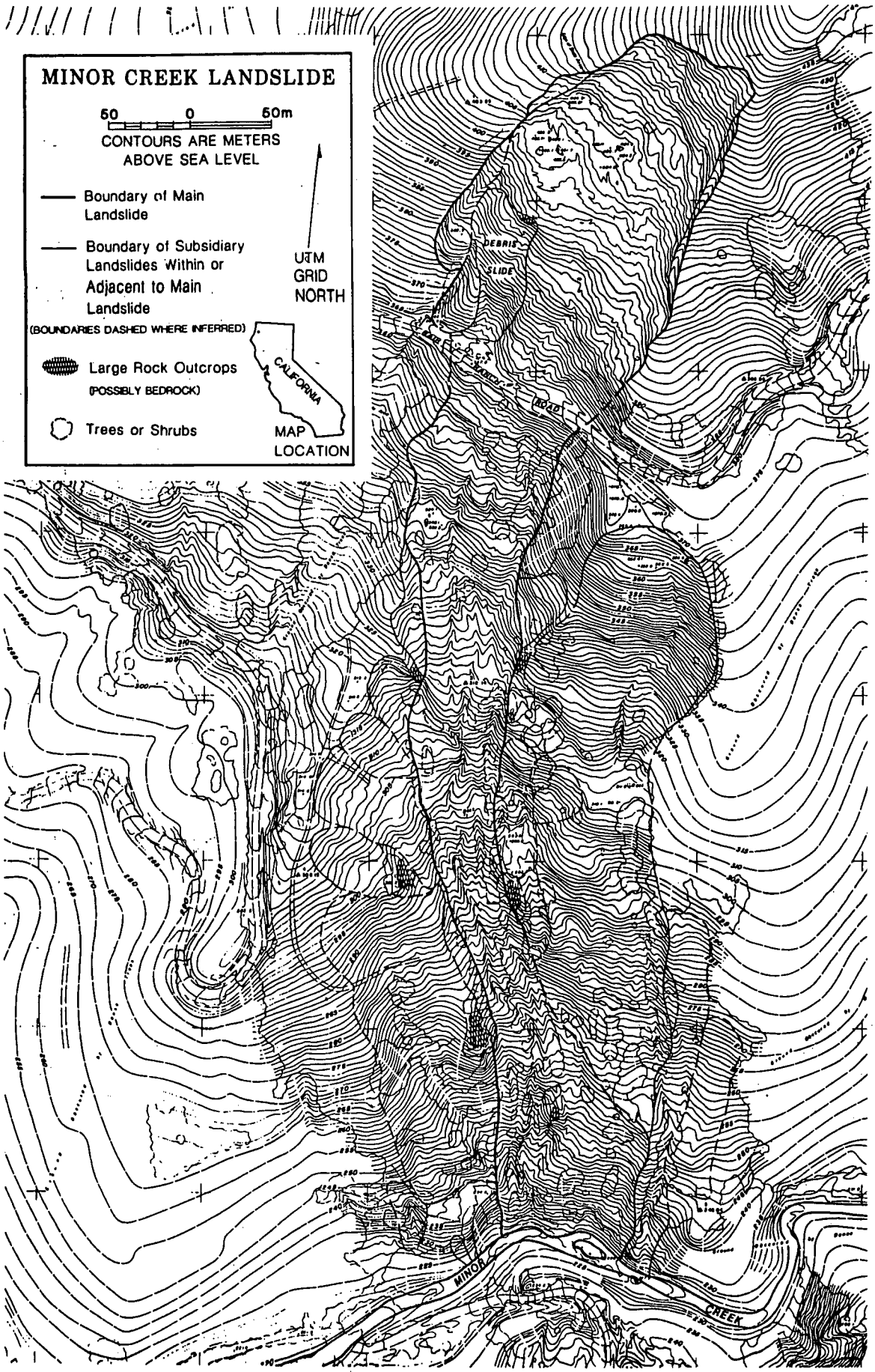

Figure 24. Topographic map of Minor Creek landslide. Photogrammetric topographic mapping was done to U.S.G.S. national mapping standards from aerial photographs taken on July 13, 1982. Morphological mapping was done in field during 1982 and 1983.

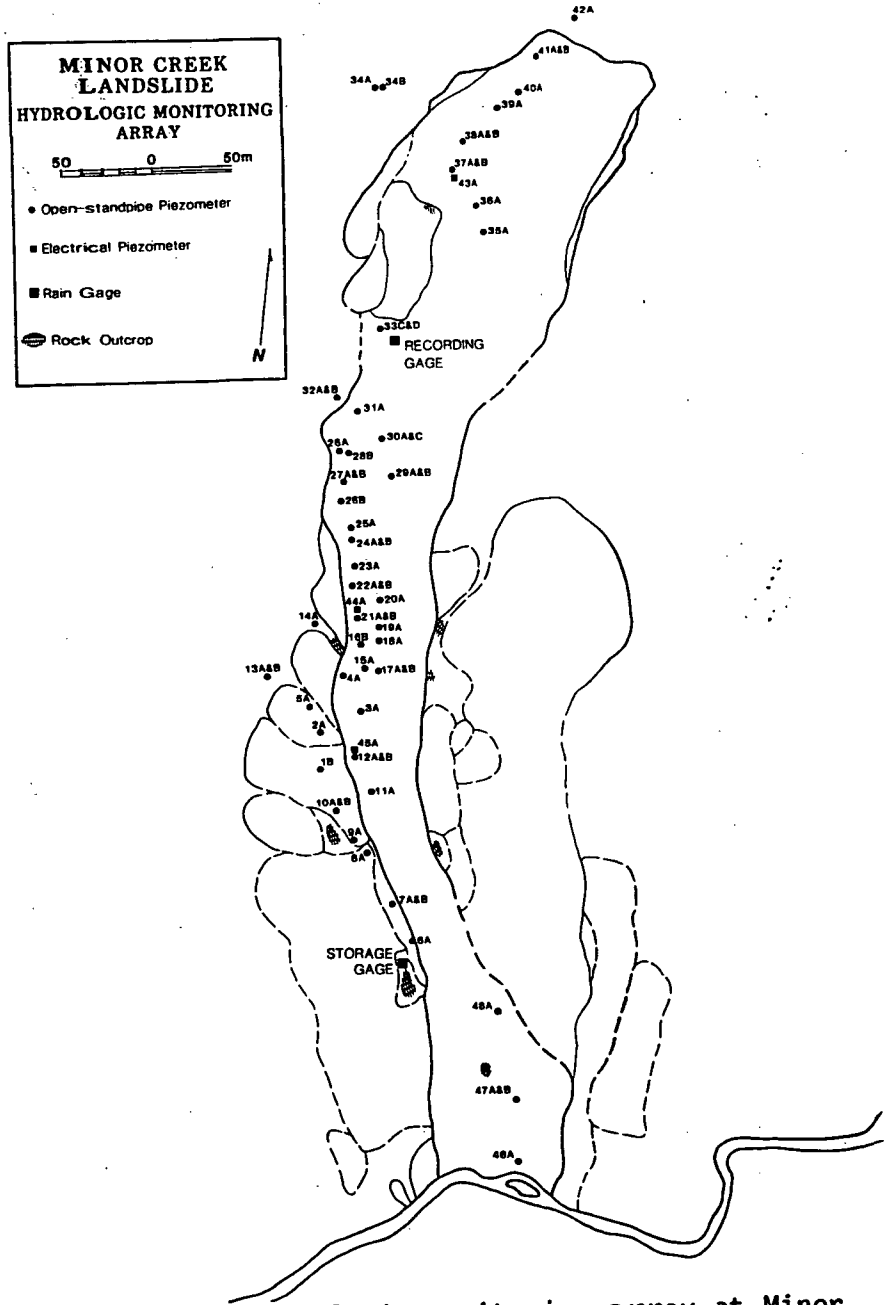

Figure 25. Hydrologic monitoring array at Minor Creek landslide, 1984.

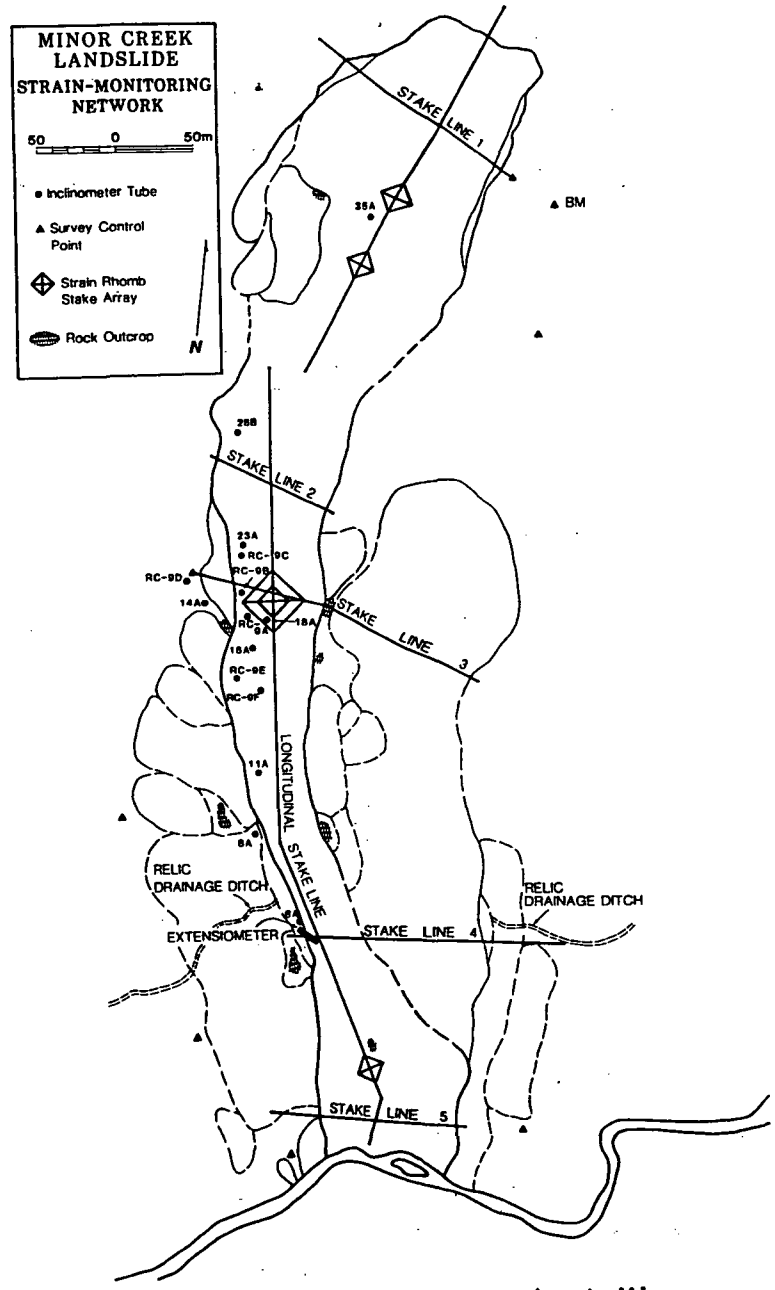

Figure 26. Strain monitoring network at Minor Creek landslide, 1984.

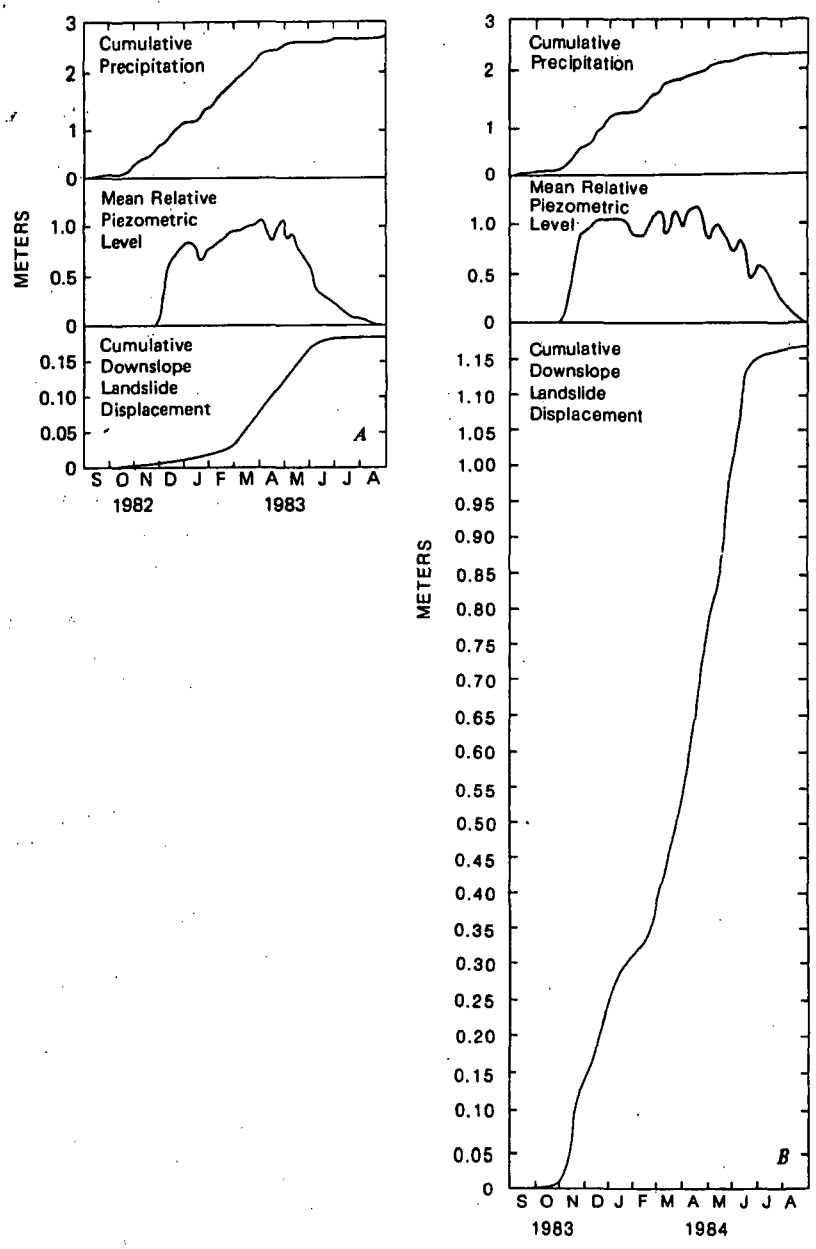

Figure 27. Temporal patterns of precipitation, piezometric response, and surface displacement at the extensiometer site, Minor Creek landslide, during two movement seasons. Piezometric levels are referenced to a datum 2.1 m below the ground surface.

Some typical vertical velocity profiles inferred from the inclinometer surveys are shown in Figure 28. These profiles show that subsurface deformation in the main body of the landslide occurs principally in a basal shear zone that averages roughly one meter in thickness and five meters in depth. Some creep deformation occurs above the basal shear zone, both in the main landslide and outside its margins. Sampling, inspection, and testing of the shear zone material shows that it differs little from the surrounding material. The lack of distinctive shear zone material and the shape of the landslide velocity profiles are both consistent with viscoplastic or pseudoplastic continuum material behavior.

Figures 29, 30, and 31 depict the surficial components of landslide displacement measured at transverse stake lines 1, 3, and 5 from the time of their installation (1973 or 1974) through April, 1984. An intriguing aspect of the displacement patterns shown in Figures 29, 30, and 31 is that the timing and amount of displacement varies along the length of the landslide. The upper portion of the landslide moved rather slowly and steadily for ten years (Fig. 29), while midslope portions of the landslide underwent movement pulses during the 1973-1974 and 1983-1984 seasons (Fig. 30). The toe of the landslide, in contrast, accelerated dramatically throughout the early 1980's, with very large displacements that culminated in 1982-1983 (Figure 31). These large displacements were catalyzed by transient undercutting of the landslide toe by Minor Creek. It appears clear, therefore, that the landslide does not translate downslope as a rigid body. Instead, different parts of the landslide respond to a variety of impetuses at different rates and different times.

Further evidence of the nonuniform motion of Minor Creek landslide is depicted in Figure 32 which shows the distribution of strain measured along the longitudinal stake line during 1982-1983 and 1983-1984. In response to the culmination of landslide toe undercutting by Minor Creek, very large extensional strains occurred near the toe in 1982-1983.

The overall movement pattern of Minor Creek landslide is summarized in Figure 33. This figure illustrates the spatial distribution of downslope sediment flux through Minor Creek landslide during the movement cycles of 1981-1982, 1982-1983, and 1983-1984. Sediment fluxes were calculated from stake-line data, inclinometer data, and field mapping data, and they may be in error by as much as 50%. Despite this considerable potential for error, Figure 33 clearly shows that major disparities exist between sediment fluxes in different portions of the landslide. These disparities appear to result from transient, nonuniform loading phenomena like fluvial undercutting of the landslide toe and spatially varied ground-water flow. Responses of the landslide to such phenomena are strongly time- and space-dependent. This reinforces the idea that Minor Creek landslide, and probably many other landslides, cannot be viewed as classic Coulomb sliding bodies. Instead, a complex suite of viscous and plastic rheological components must be considered in assessing landslide behavior.

From this vantage point, the inner gorge slopes in the upstream part of Redwood Creek basin can be seen. Project the long, visible slopes

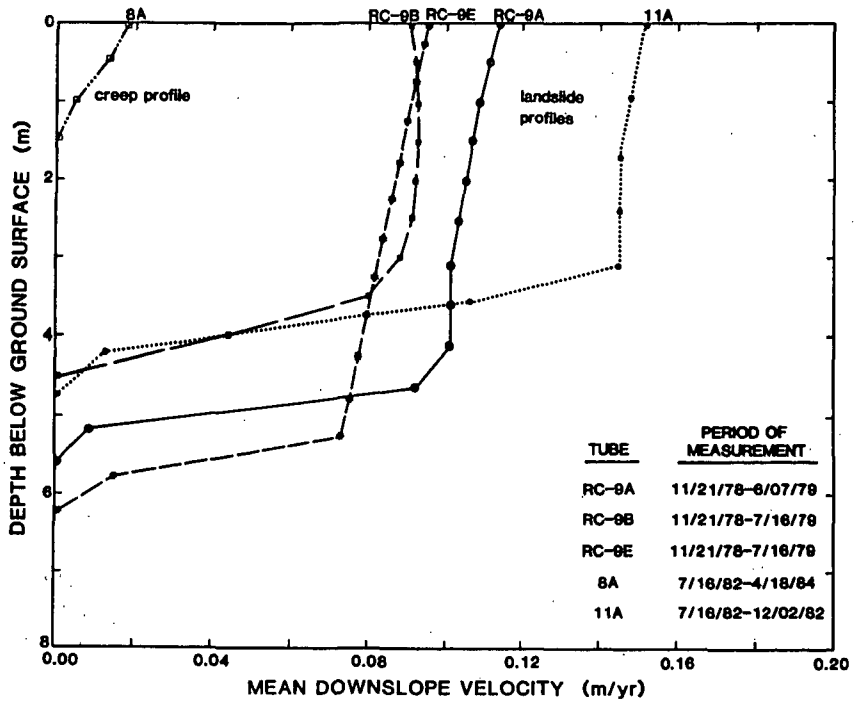

Figure 28. Representative vertical velocity profiles inferred from repetitive inclinometer surveys of bore-hole casing displacement, Minor Creek landslide.

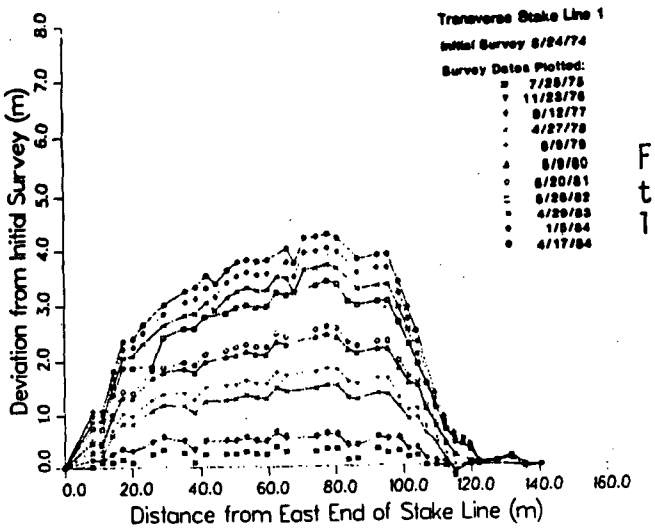

Figure 29. Surveyed displacements of transverse stake line 1, Minor Creek landslide.

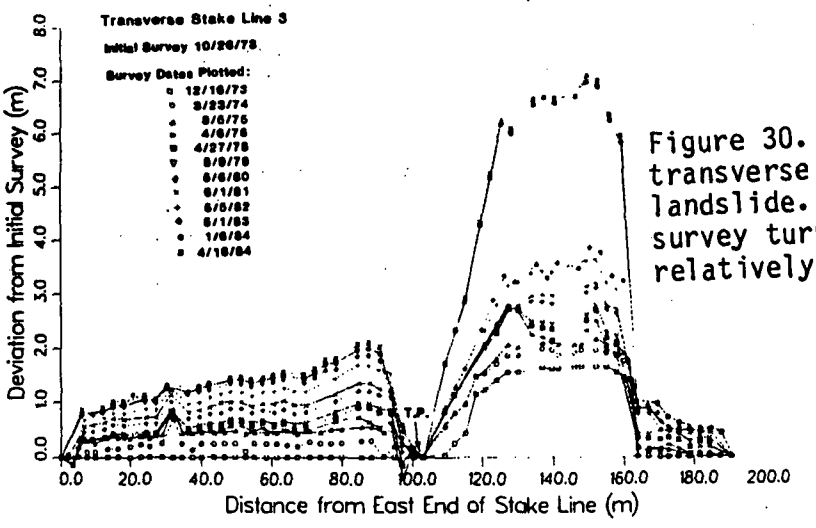

Figure 30. Surveyed displacements of transverse stake line 3, Minor Creek landslide. The point marked "T.P." is a survey turning point situated on a relatively stable rock outcrop.

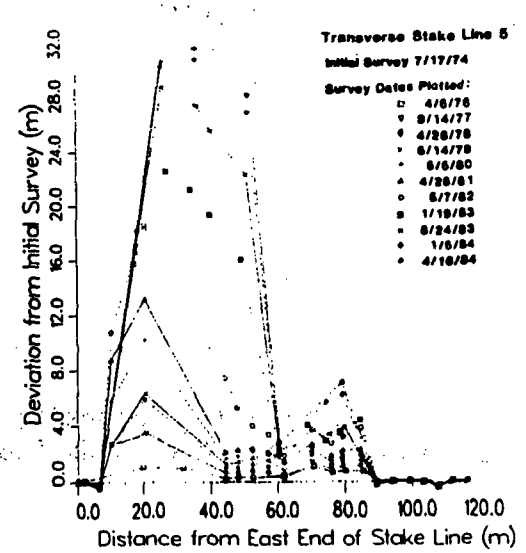

Figure 31. Surveyed displacements of transverse stake line 5, Minor Creek landslide.

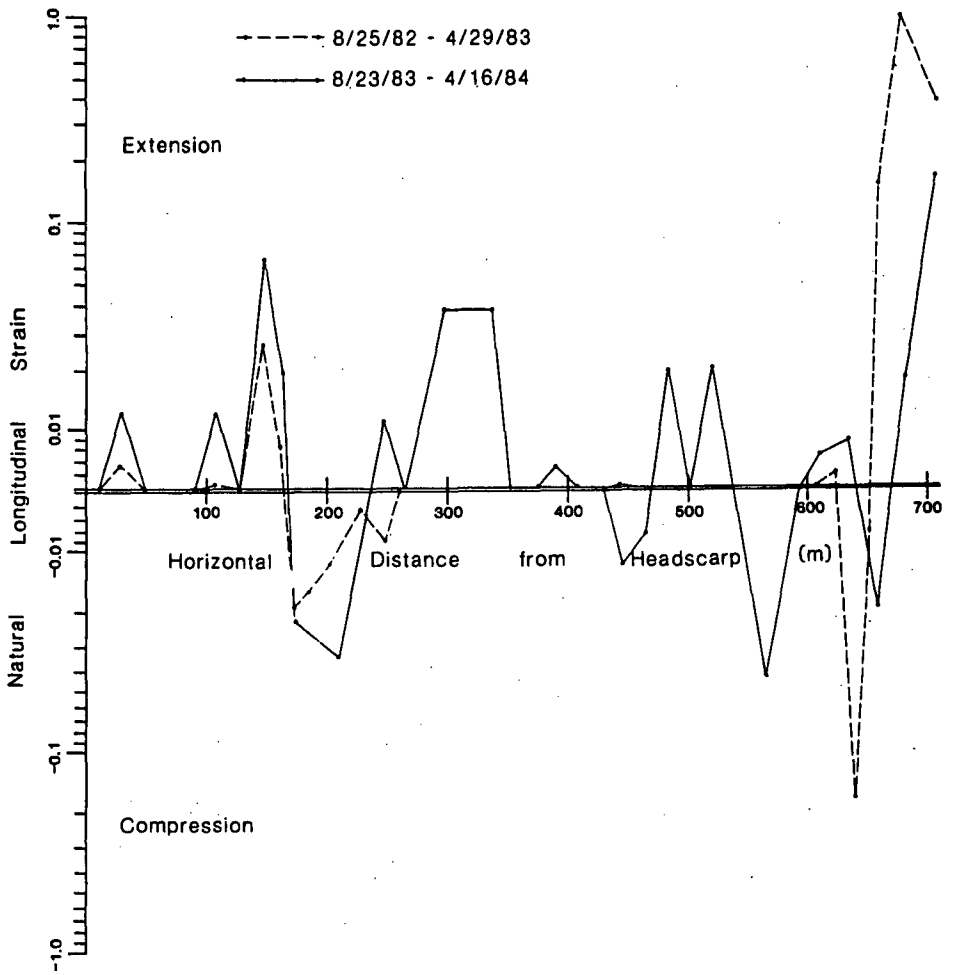

Figure 32. Distribution of measure longitudinal strains along the longitudinal stake line, Minor Creek landslide. Strains smaller than 0.005 are not plotted because strain measurement errors could be as large as 0.005.

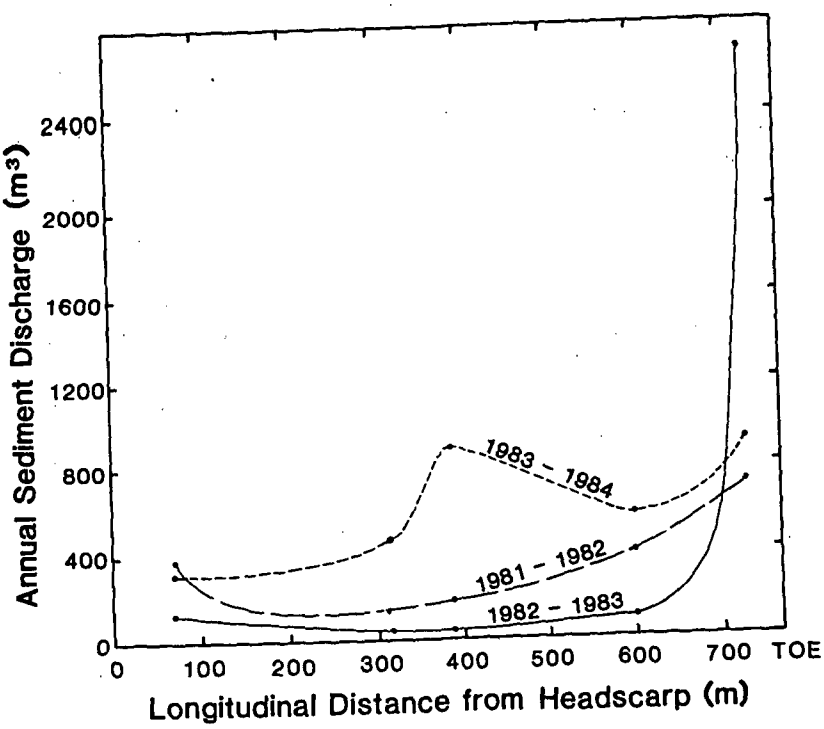

Figure 33. Spatial distribution of downslope sediment flux through Minor Creek landslide during three movement seasons.

toward each other and note that they intersect in the air, above the stream channel. Inner gorge slopes are formed below this point of intersection and can be just barely seen from this view (Fig. 34). Some of the inner gorge slopes visible from here are sites of debris slides: this is presumably the major process that forms such slopes.

The term "inner gorge" was first used by Clarence E. Dutton (1882) in his descriptions of the Grand Canyon. Francois Matthes (1930) applied the term to slopes above Yosemite Valley and the term has been subsequently applied to slopes in north coastal drainage basins in California by Farrington and Savina (1977), and Furbish and Rice (1983). In an inner gorge, slopes directly adjacent to the channel are steeper than those further up the hillslope. A clearly defined break-in-slope separates the steeper inner gorge slopes from the more moderate, higher hillslopes. Inner gorge slopes do not appear to have one common angle, and slope steepness probably depends in large part on the underlying rock type. A full account of the morphology and genesis of inner gorge slopes in the Redwood Creek basin is given by Kelsey (in press).

We plan to leave Stop 1 at 10:30 a.m. Retrace route to west end of Highway 299.

46.2 Junction 299 and Highway 101. Take 101 North. For the next 1.4 miles the highway crosses alluvial flats at the mouth of the Mad River.

47.6 Mad River crossing. See yesterday's road log for the story of this river's elegant name. The lowermost Mad River flows in a structural trough. On the north side of the valley is graywacke brought up along a reverse fault. The Mad River trough formed on the downthrown side of one of a series of tilted blocks produced by reverse faulting in the Mad River Fault Zone (see road log for third day).

49.3 School Rd. Exit. The flat surface along which we have been travelling is a marine terrace surface called Dows Prairie. Both the Arcata Airport and McKinleyville lie on this surface. They are separated by a northwest trending scarp that proved, on trenching, to be produced by a high-angle reverse fault. This fault is the northernmost of seven reverse faults between here and central Arcata, which together comprise the Mad River Fault Zone (Carver, et. al., 1983). We will see an exposure of one of these faults on the third day of the conference.

The town of McKinleyville was first called Dows Prairie, then Minorville, after one Isaac Minor, who founded the town. Minor changed the town's name to McKinleyville after the 1901 assassination of the president. Minor's name is still applied to the Minor Creek, the tributary of Redwood Creek that we visited earlier today.

51.7 At Arcata Airport exit, look east (right) to see a Holocene fault scarp (not to be confused with the airport runway, just to the northwest). Until recent work (Woodward-Clyde consultants, 1980) established that this and similar scarps were indeed tectonic, most people believed that they were marine terrace scarps.

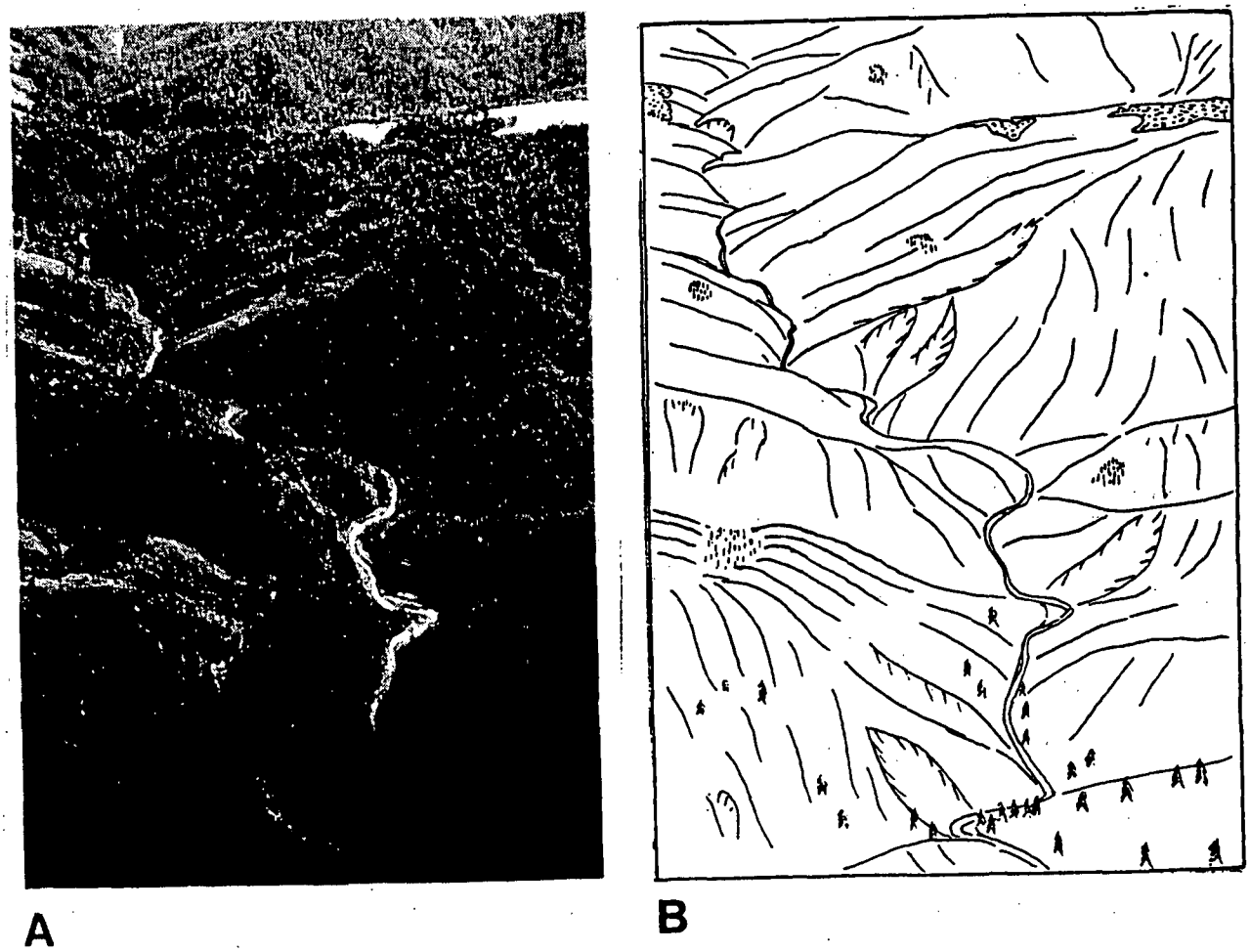

Figure 34. Oblique aerial photo (A) and accompanying sketch based on the photo (B) looking upstream at a 12 km reach of the Redwood Creek basin in the upper third of the watershed. The inner gorge is well developed along this reach of Redwood Creek.

From here, the road descends from the marine terrace to Clam Beach. Trinidad Head, visible ahead to the west, is underlain by an intrusive complex of diorite, keratophyre, tonalite, etc. It is a block in the Franciscan melange. Trinidad Head is attached to the mainland by a marine terrace. Sea stacks on the modern marine platform are visible south of Trinidad Head. Between Trinidad Head and Patricks Point, the coast is formed on Franciscan melange with at least seven distinct terrace levels rising to the east inland. These terraces have been warped into an east-west trending anticline (see Figs. 35 and 36, from Stephens, 1982). Both the heavy vegetation and the fact that the highway was constructed without attention to geologic points of interest make it impossible to discern the terrace steps from the road.

53.9 Highway is constructed across Holocene dunes in Clam Beach, visible on the west side of the road.

55.1 Vegetated dunes are visible to the west near the Crannell Road exit. Most dunes trend northwest and formed in response to winter winds from the southwest.

55.2 Little River crossing

56.1 Melange and Crannell dune sands are exposed in roadcuts along highway. Relief visible from road is produced by the marine terrace scarps, but pattern of scarps is obscured.

58.8 Trinidad exit. Trinidad is the oldest town in the Humboldt Bay area. It was used as a harbor until Humboldt Bay was rediscovered, and was even incorporated as the county seat of "Klamath County." However, soon after the rediscovery of Humboldt Bay, the bulk of shipping and commerce moved south and Trinidad was all but abandoned.

59.3 Sea stacks have been preserved on some of the old terraces, now uplifted above sea level. One such stack is Strawberry Rock, composed of greenstone, which can be seen to the east.

64.1 Patricks Point turnoff. Patricks Point State Park is on the lowest marine terrace and contains a number of preserved sea stacks.

64.6 Sands in roadcuts. The magnitude of Quaternary deformation in this area is well illustrated by the fact that the marine terrace the road is built on here is about 100 to 150 m high and tilts down to sea level in the next few miles. Unconformities within the terrace deposits show the progress of the tilting.

65.9 Big Lagoon exit. Big Lagoon is almost totally unaltered except for the causeway built for Highway 101. During most winters, the lagoon fills and the spit breaches one to four times, depending on the runoff from Maple Creek. Most of the breaches occur at the north end of the spit. When the spit breaches, the lagoon empties in less than one day and the breach remains open anywhere from a day to a week before winter waves rebuild a berm across the breach. Stone Lagoon to the north behaves in the same way, but its spit does not breach as often because of the smaller drainage

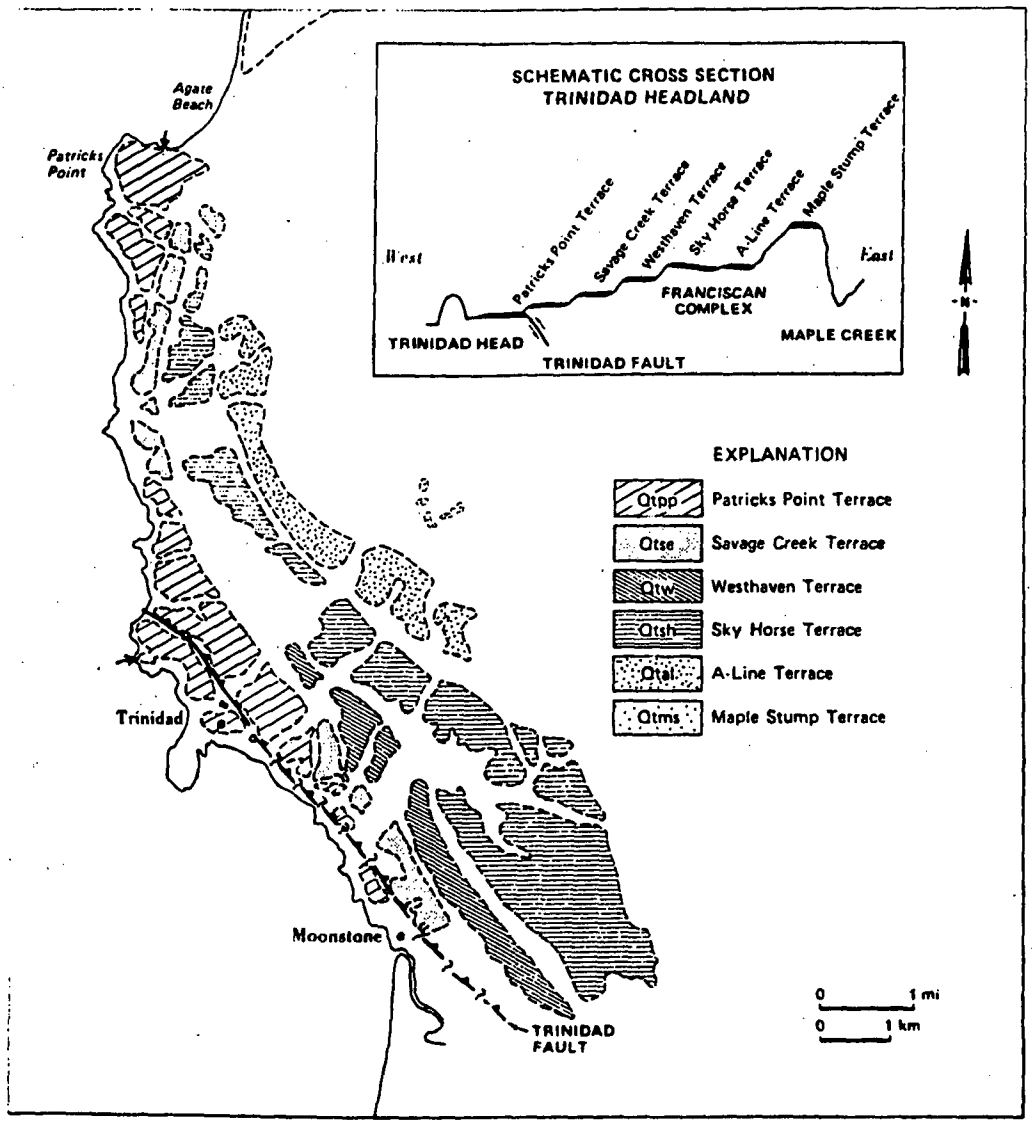

Figure 35. Map of Late Quaternary marine terraces on the Trinidad Headlands. From Stephens, 1982.

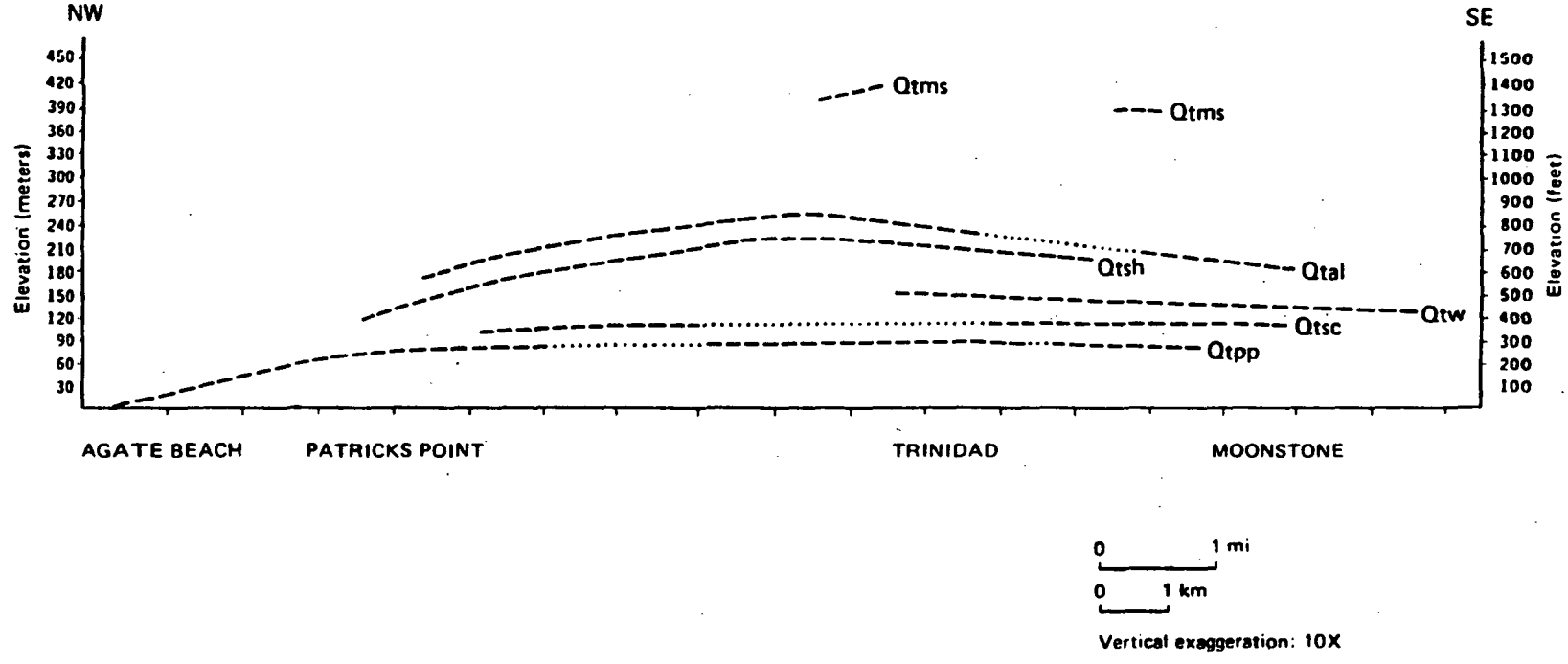

Figure 36. Longitudinal profiles of marine terraces on the Trinidad Headlands. From Stephens, 1982.

basin supplying the lagoon with water. Big Lagoon apparently formed within a structural depression similar to the one at the lower end of the Mad River. The controlling structure is the Big Lagoon Fault, a high angle reverse fault that offsets Neogene sediments that blanket the Franciscan melange to the east of Big Lagoon. The Big Lagoon Fault parallels the northwest side of the lagoon.

66.2 Freeway ends. The road in this area follows the trace of the Big Lagoon Fault. The 1981 earthquake, centered offshore, caused sand volcanoes and other liquefaction features along the lagoon side of the Big Lagoon spit.

70.3 Divided highway begins.

71.4 You may be able to catch a glimpse of Dry Lagoon to the west (left).

71.7 End of divided highway.

73.4 At about this place, the highway crosses the Bald Mountain Fault, separating Franciscan melange on the south from Redwood Creek schist on the north.

73.9 Stone Lagoon to west.

76.2 Highway traverses spit of Freshwater Lagoon. The lagoon has a very small drainage area. Even before the highway was built across the Freshwater Lagoon spit, the spit almost never breached, which probably accounts for the name of the lagoon.

76.6 New visitors center, Redwood National Park, at south end of Redwood Creek beach.

78.5 Road crosses lower Redwood Creek. Note levees along both sides of the Creek. The levees extend from the mouth of the creek to the head of the bottom lands approximately four km upstream.

We are entering the town of Orick, which used to be supported exclusively by logging until the creation of the National Park. Now, tourism is one of the major sources of income. All of the forested hillslope land visible from the road is within Redwood National Park, but the bottomlands occupied by the town of Orick and the prairies to the northwest are entirely privately owned.

78.6 Left turn onto road marked "Coastal Access". Follow fishing signs to parking at estuary. Note that the last downstream meander of Redwood Creek was bypassed during channelization.

80.5 STOP 2 - MOUTH OF REDWOOD CREEK - LUNCH STOP

Figure 37 shows the location of the afternoon stops.

Before lunch, Cindy Ricks will discuss the dynamics of the Redwood Creek estuary, including the effects of the levees on sediment transport and deposition in lower Redwood Creek and the estuary.

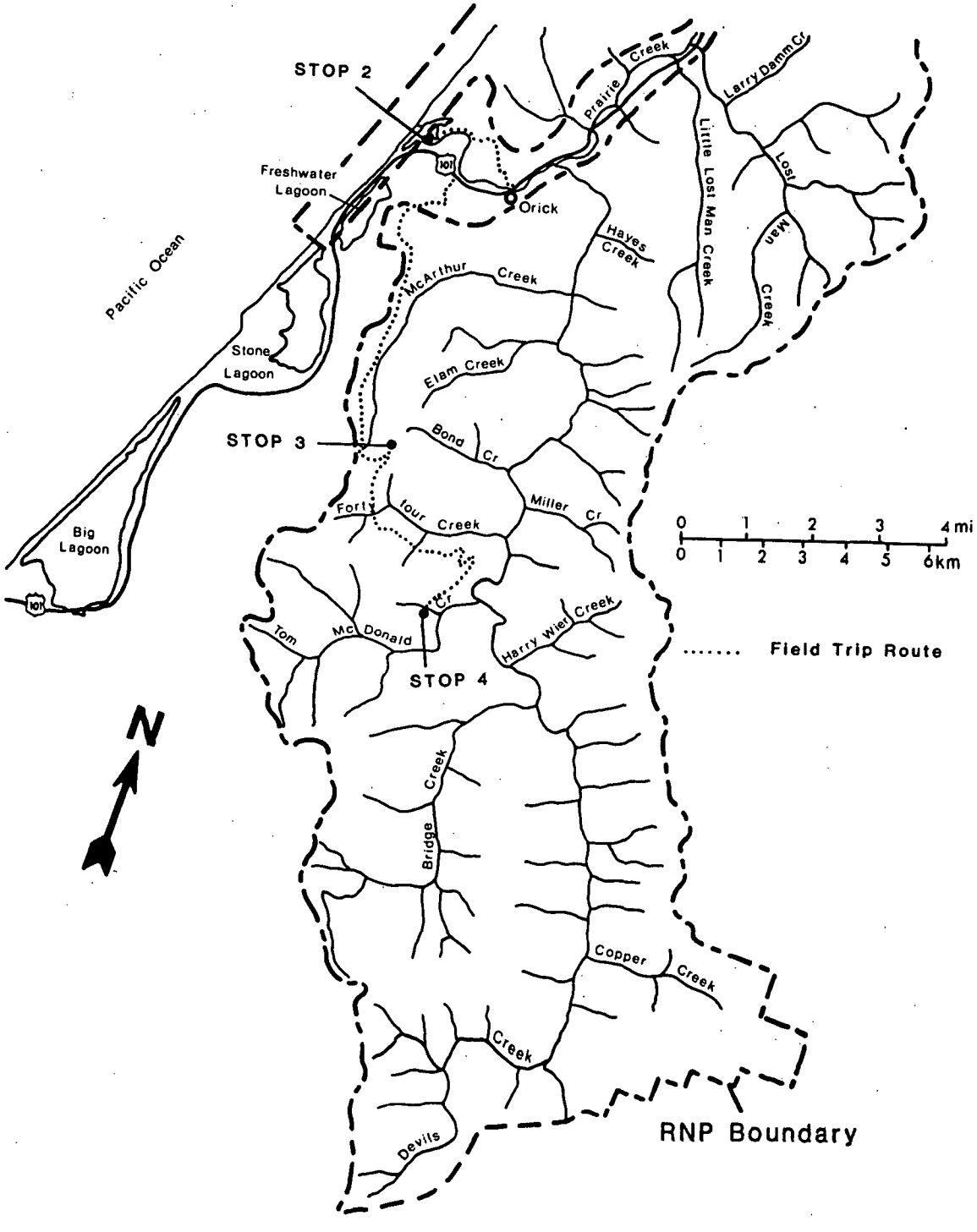

Figure 37. Map of the lower Redwood Creek basin showing location of field trip route and stops within Redwood National Park.

I. REDWOOD CREEK ESTUARY, By Cynthia Ricks

Since the early 1950s, the distribution of sediment at the mouth of Redwood Creek has been altered by the effects of channel aggradation and channelization along the lower reach. Severe flooding in 1953, 1955, and 1964 caused bank erosion, landsliding, and channel geometry changes along Redwood Creek. The increased sediment load resulted in channel aggradation and widening along the lower floodplain (see Fig. 38). Prior to 1966, floods scoured the north slough, middle slough, and main channel, thus maintaining a hole adjacent to the north cliffs at least 20 feet deep. The December 1964 flood scoured the entire beach from the north cliffs south to the former Cal-Pacific Mill site. Floods generally deposited material across the floodplain from the confluence with Prairie Creek to the middle island. Flood damage in the town of Orick prompted channelization of Redwood Creek in 1966-1968. The distribution of erosional and depositional sites at the mouth has been more drastically altered by the effects of channelization than of aggradation.

As we drive along the south levee toward the mouth of Redwood Creek, note the last downstream meander which was bypassed and isolated from the main channel of Redwood Creek during channelization. Channelization was accompanied by removal of bed roughness elements, shaping a trapezoidal channel with an increased hydraulic radius, and steepening the channel gradient. This caused an increase in the mean velocity and frequency of mobilization of the substrate between the levees. With streamflow confined between the levees, sediments deposited in the last downstream meander (south slough) and north slough are no longer flushed from the mouth of Redwood Creek. Since 1966, 47 to 54 percent of the lower estuary (between zero and four feet above mean sea level) has filled with sediment or become isolated from the embayment (see Figures 39 and 40).

Sediment yield of Redwood Creek is among the highest for a basin of its size in North America, but under present conditions fluvial sediment is not accumulating at the mouth. Heavy mineral and textural data indicate that during high to moderate streamflow, sand- and gravel-sized sediment is flushed through the embayment. Overwash across the storm berm and tidal current transport are the dominant processes of deposition in the sloughs, delivering marine sediment to the estuary.

Sediment accumulation has also altered the seasonal sequence of migration and closure of the outflow channel which determines the embayment water volume, substrate distribution, and water quality during the low flow period from spring to early fall. Since the volume of water subject to tidal fluctuations (tidal prism) has decreased, the ebb tide current velocity has also decreased, resulting in earlier migration and closure of the outflow channel. When the rates of outflow, seepage, and evaporation do not exceed the stream discharge, the embayment expands, becoming connected with the productive north and south sloughs (Figure 41). More frequent closure and flooding of backwater areas and adjacent pastures has historically led to artificial breaching of the berm. In the past, such premature breaching released 75 percent of the embayed water volume being used by 20,000 juvenile salmonids for summer rearing habitat.

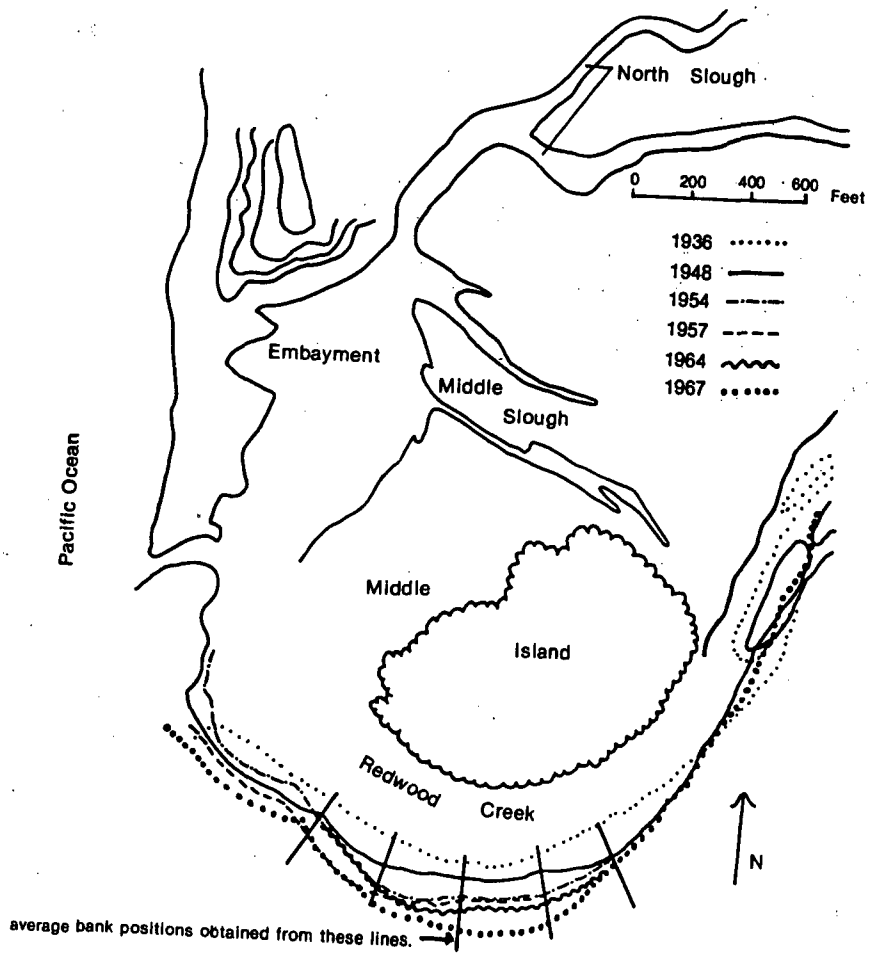

Figure 38. Bank positions along the last downstream meander of Redwood Creek, 1936-1967. Figure from Ricks, in press.

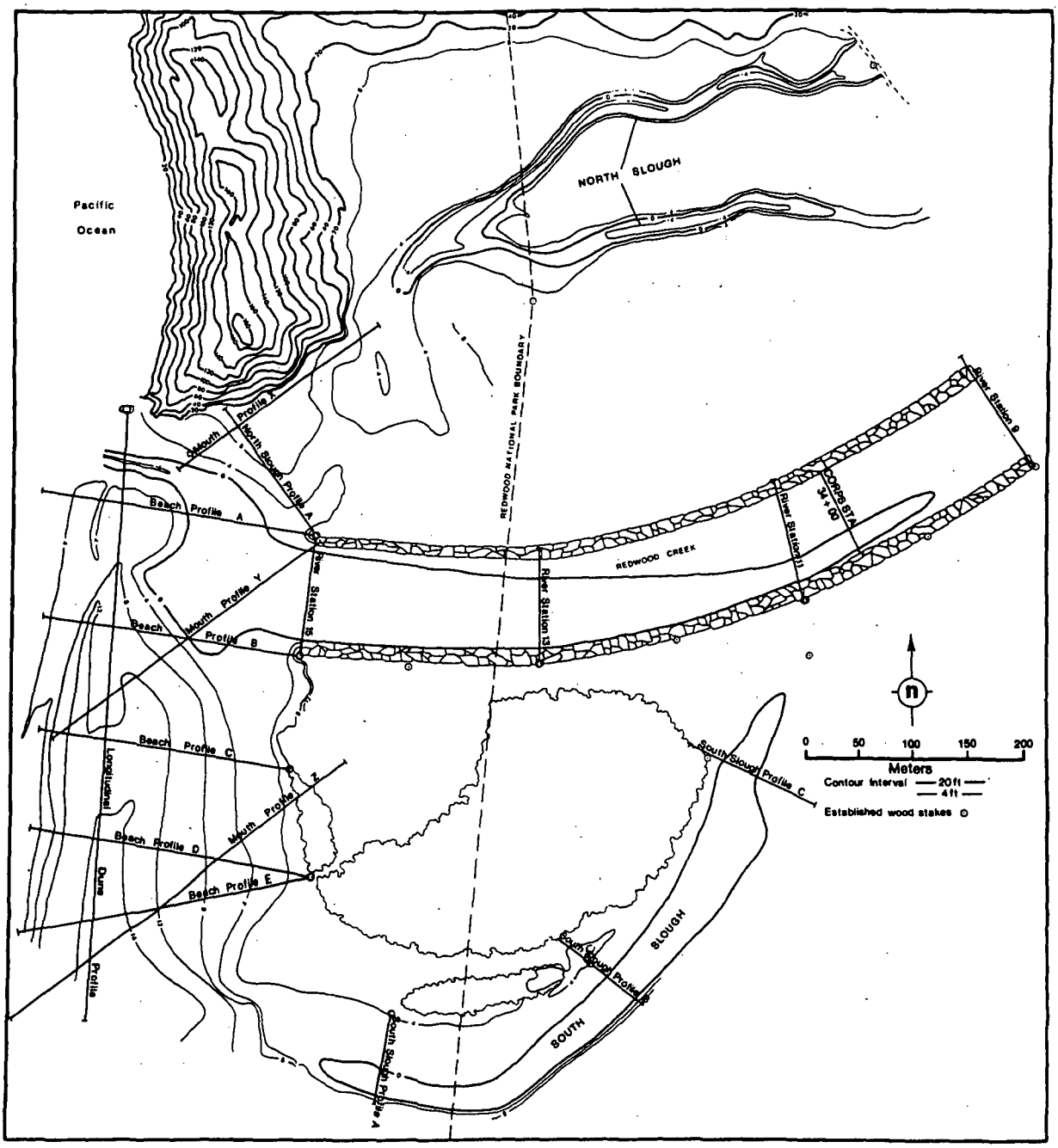

Figure 39. Profile locations for cross-sections at the mouth of Redwood Creek. Figure from Ricks, in press.

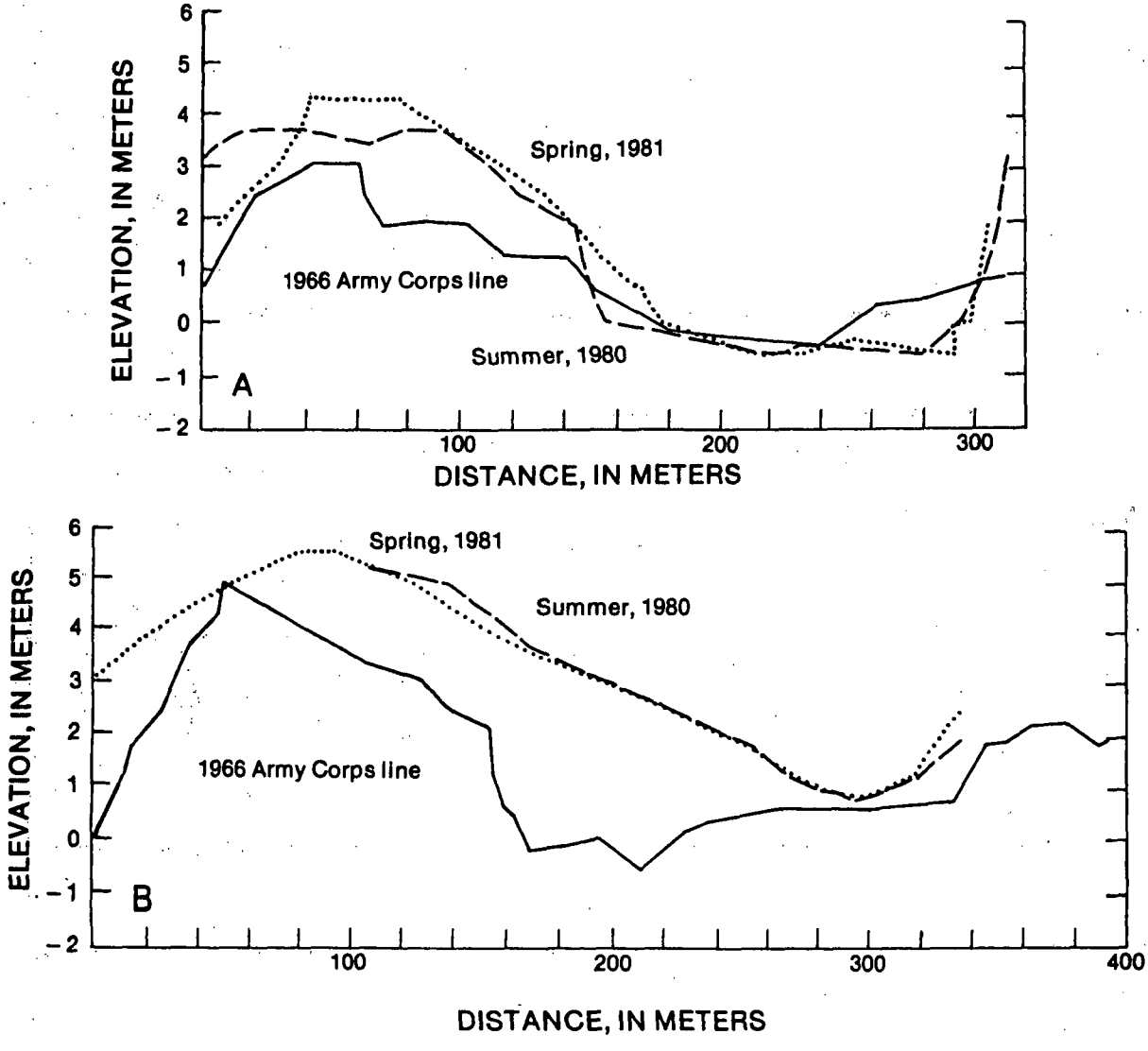

Figure 40. Topographic profiles across the mouth of Redwood Creek. Both profiles run from SW to NE across the longitudinal dune into the embayment. Top (A), mouth profile Y. Bottom (B), mouth profile Z. Profile locations on Figure 39. Figure from Ricks, in press.

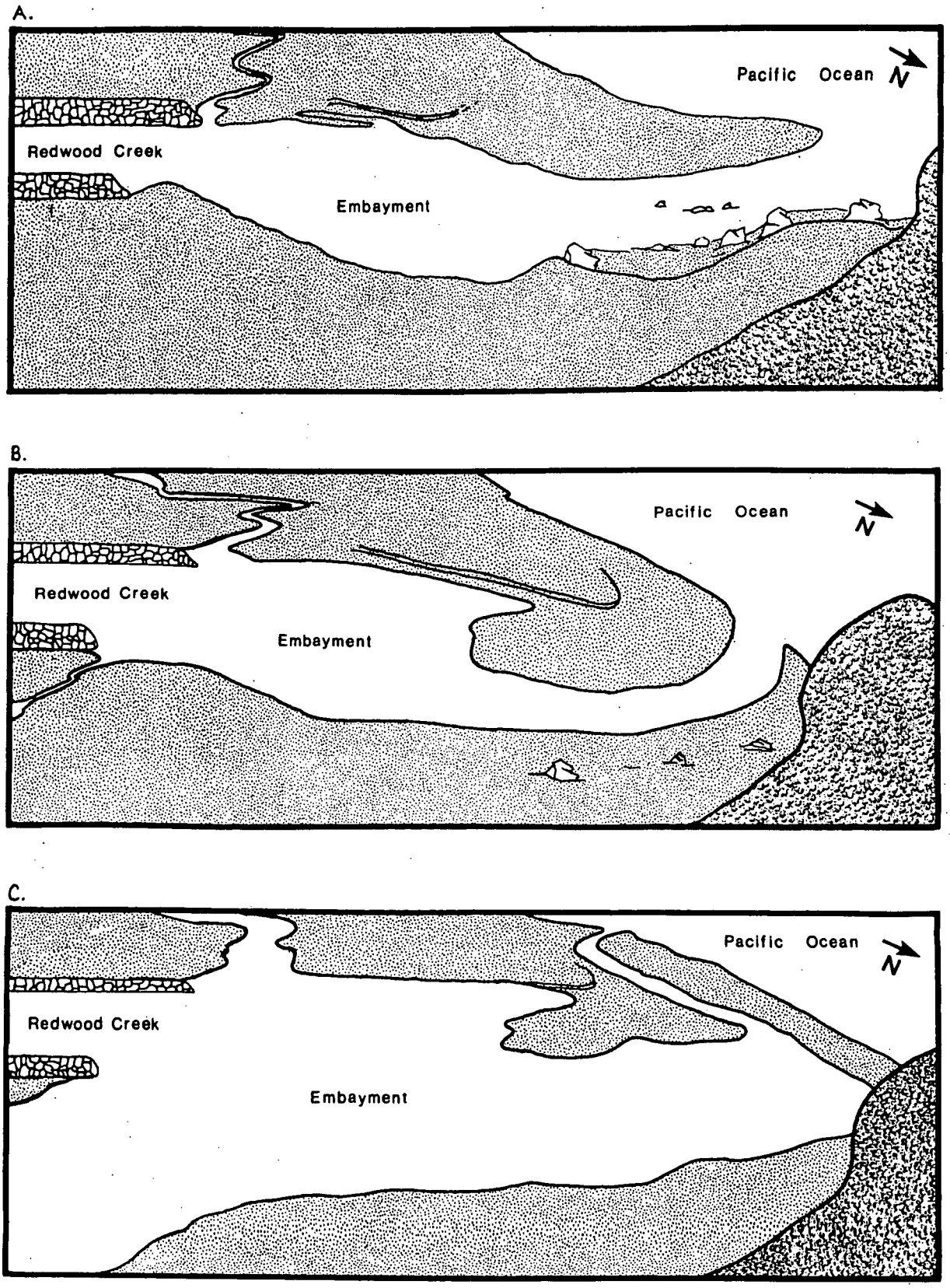

Figure 41. Mouth of Redwood Creek: oblique views from the top of the north cliffs looking to the south. A, January 12, 1980. B, April 19, 1980. C, June 14, 1980. Figure from Ricks, in press.

II. MAGNITUDE AND DYNAMICS OF SEDIMENT STORAGE IN REDWOOD CREEK (From Madej, 1984)

We have now seen Redwood Creek at a mid-basin location (the upper end of Redwood Valley) and we have seen the Redwood Creek channel in its lowermost reaches at the channelized estuary. Mary Ann Madej, geologist for Redwood National Park, has conducted extensive studies of the magnitude and dynamics of sediment storage along the 105 km long main channel of Redwood Creek and will discuss results of this investigation during the lunch stop. The following paragraphs are edited from Madej, 1984.

Storage of alluvium in the mainstem of Redwood Creek was quantified for three time periods spanning 35 years, 1947, 1964 (post-flood), and 1980. An unusual amount of aggradation occurred during the December 1964 flood (a 50-year flood), increasing the total volume of sediment stored on the valley floor by almost 1.5 times to 16×10^6 m^3. High landslide activity during the 1964 flood contributed to 5.25×10^6 m^3 to the mainstream of Redwood Creek, and channel storage increased by 4.74×10^6 m^3. Fig. 42 shows cumulative landslide input to the mainstem and deposition in the channel resulting from the December 1964 flood. Moderate to high flood flows (2 to 20 year recurrence intervals) following 1964 eroded sediment in the upper basin and redeposited it in downstream reaches. In addition, floods in 1972 and 1975 deposited sediment in downstream reaches. As a result, there was little change in the total sediment on the valley floor. This migration of a slug of sediment down Redwood Creek was easy to follow on successive resurveys of channel cross-sections along the main channel. Figure 43 shows three cross-sections from representative reaches of Redwood Creek. Cross-section 40 is located in the upper basin and shows the increase in channel bed elevation in the 1960s and a subsequent decrease to almost the 1953 level. Downcutting through sediments deposited in 1970 occurred at cross-section 25, but aggradation is still occurring near the mouth, at cross-section 6. Because of the relatively simple, elongate basin geometry of Redwood Creek compared to the Van Duzen basin, downstream movement of the locus of aggradation was straightforward in Redwood Creek, but complex in the Van Duzen River.

Presently, sediment is stored in several geomorphic compartments, and some compartments (such as recent gravel flood terraces, debris jams, stable alluvial terraces and strath terraces) are only found in particular reaches of Redwood Creek. Boundaries of the upper, middle, and lower reaches are shown in Figure 44. Figure 45 is a longitudinal profile of Redwood Creek showing the distribution of localized sediment compartments. Potential mobility of sediment stored in Redwood Creek was characterized as active, semi-active, inactive and stable, depending on its distance from and height above the thalweg, and the age and type of vegetation on the deposit. Fig. 46 a, b is a schematic cross section and plan view of these four types of sediment reservoirs in Redwood Creek.

To identify active sediment in the channel bed, the amount of scour and fill occurring during various flows was determined through scour chains and discharge measurement notes. In this gravel-bedded stream, depth of

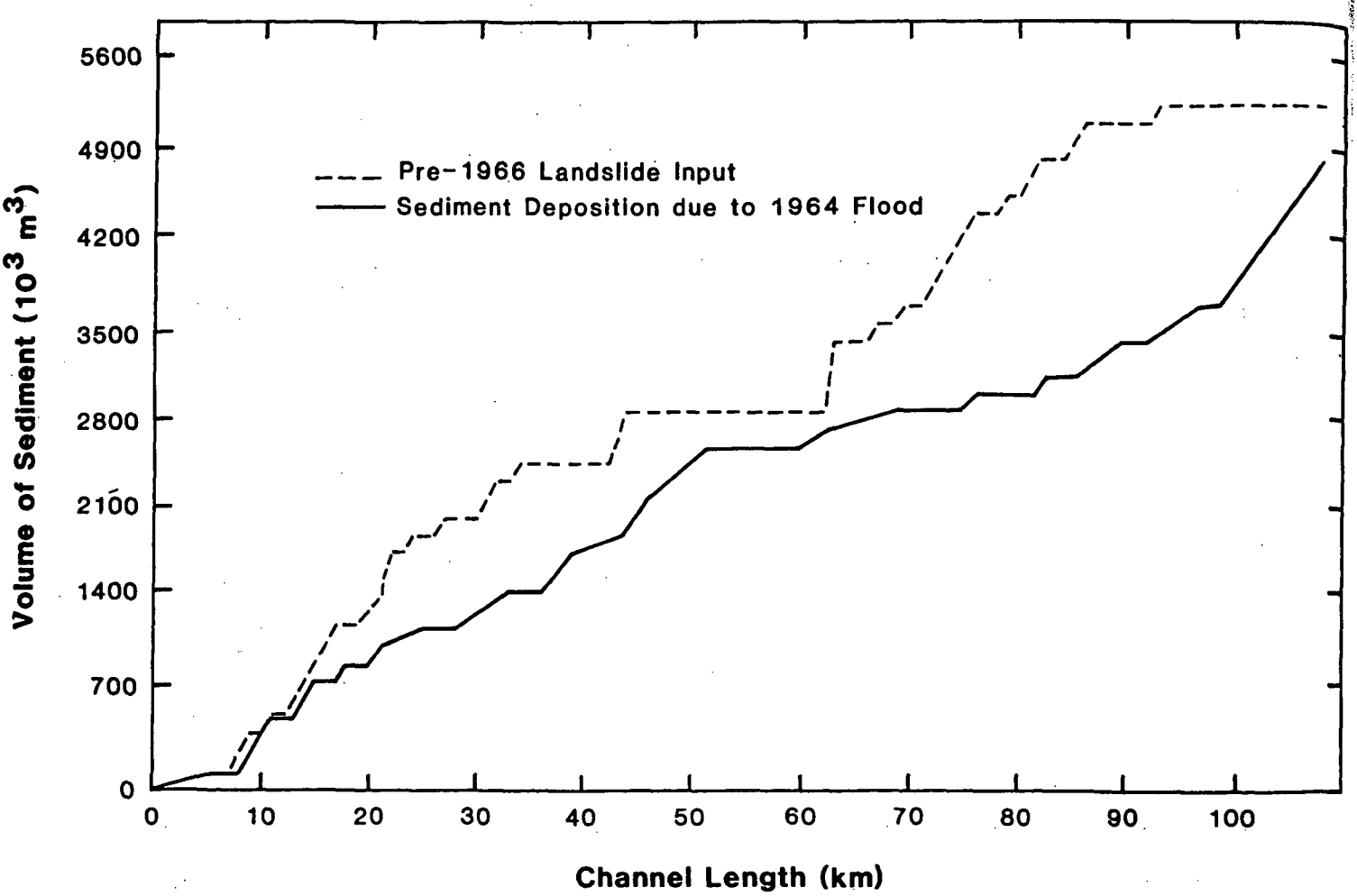

Figure 42. Cumulative volumes of total landslide input to the mainstem of Redwood Creek and the deposition in Redwood Creek resulting from the December 1964 flood. Landslide data are from Kelsey and others (in press). Figure from Madej, 1984.

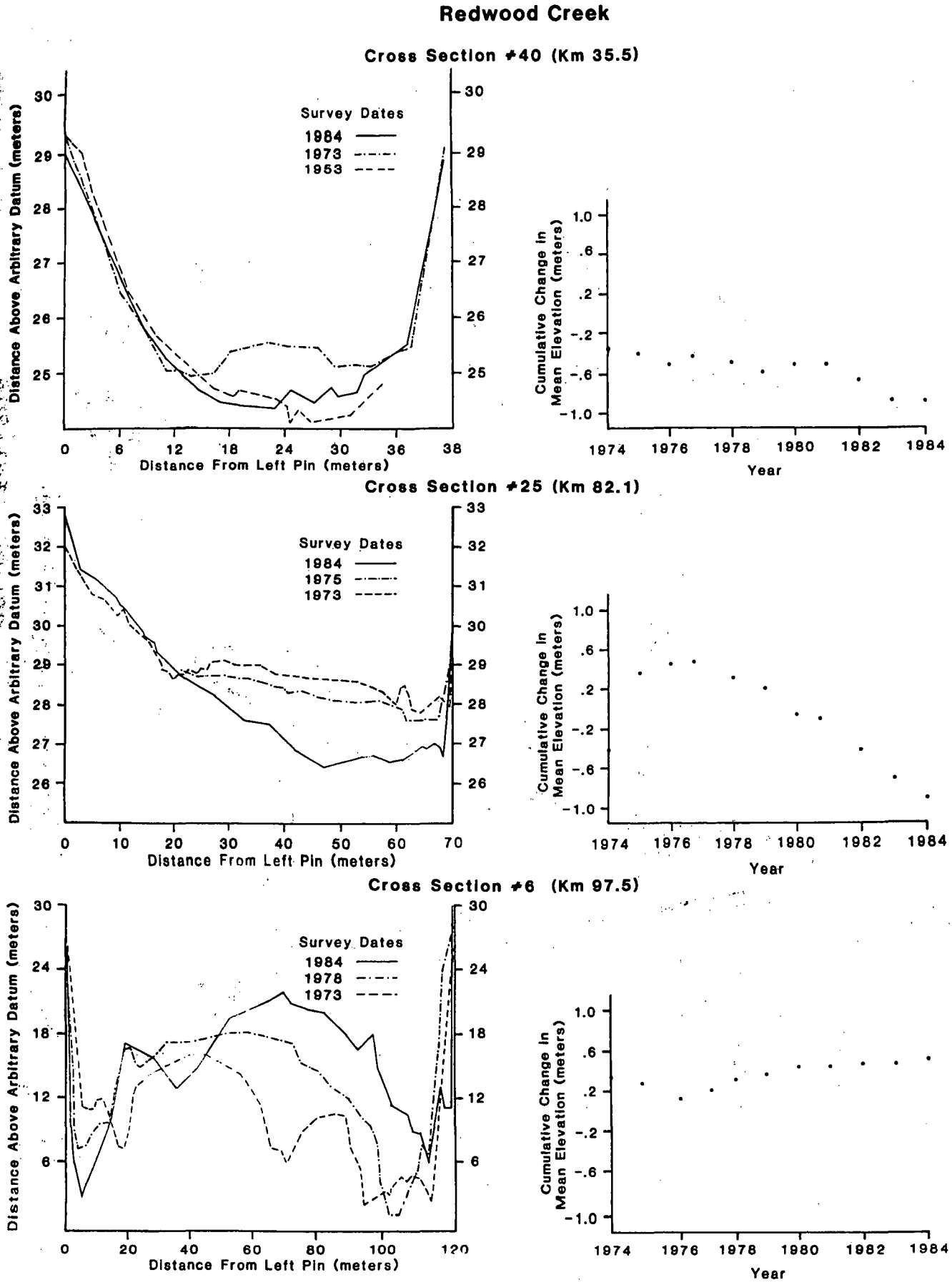

Figure 43. Cross-section surveys and cumulative changes in mean bed elevation for three stations in Redwood Creek. Cross-section 40 is in the upper third of the basin and documents progressive downcutting after aggradation. Cross-section 25 also shows consistent downcutting, whereas Cross-section 6 near the mouth of Redwood Creek shows progressive aggradation. Figure from Madej, 1984.

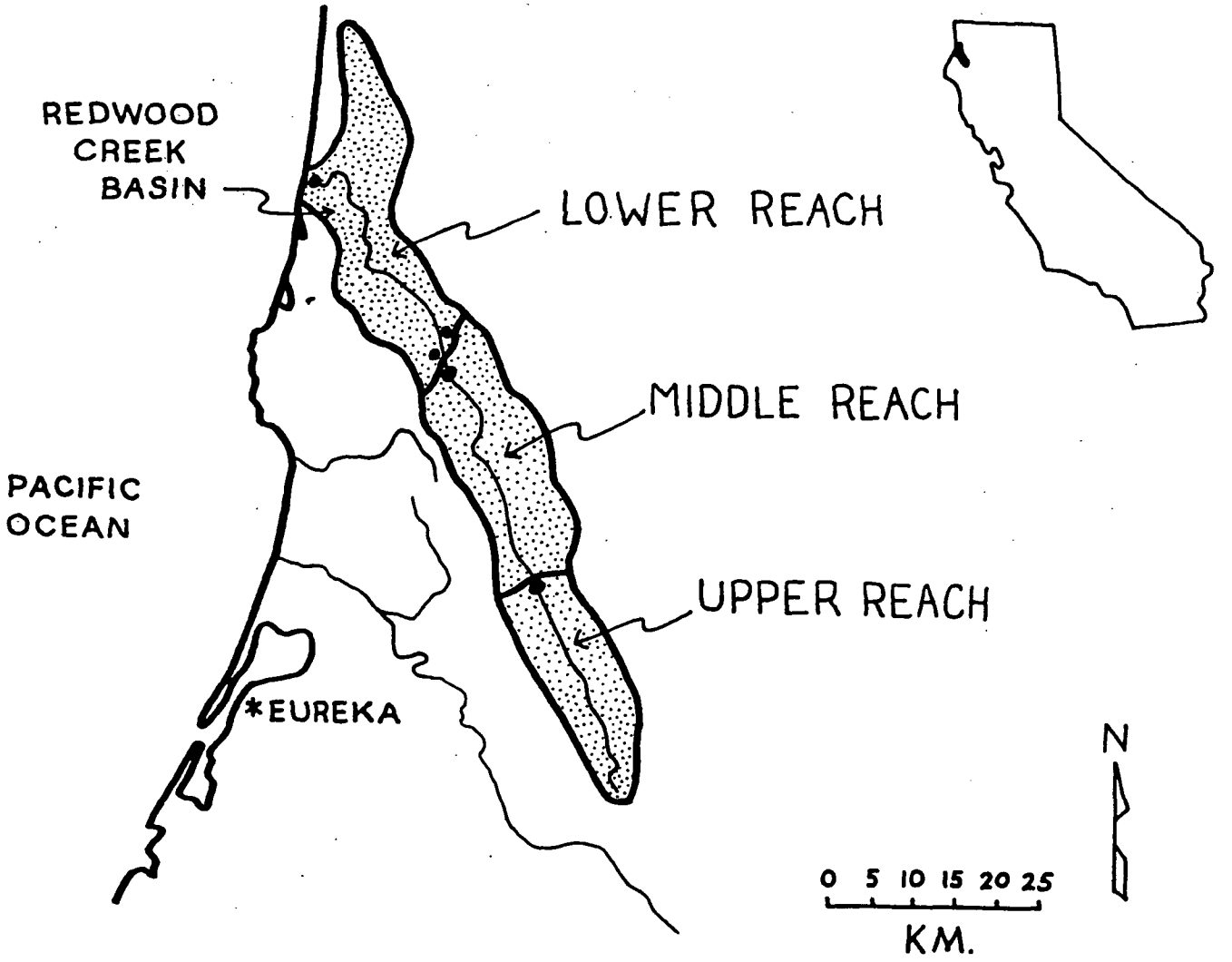

Figure 44. Sketch map of Redwood Creek showing lower, middle and upper reaches.

• = U.S.G.S. gaging stations

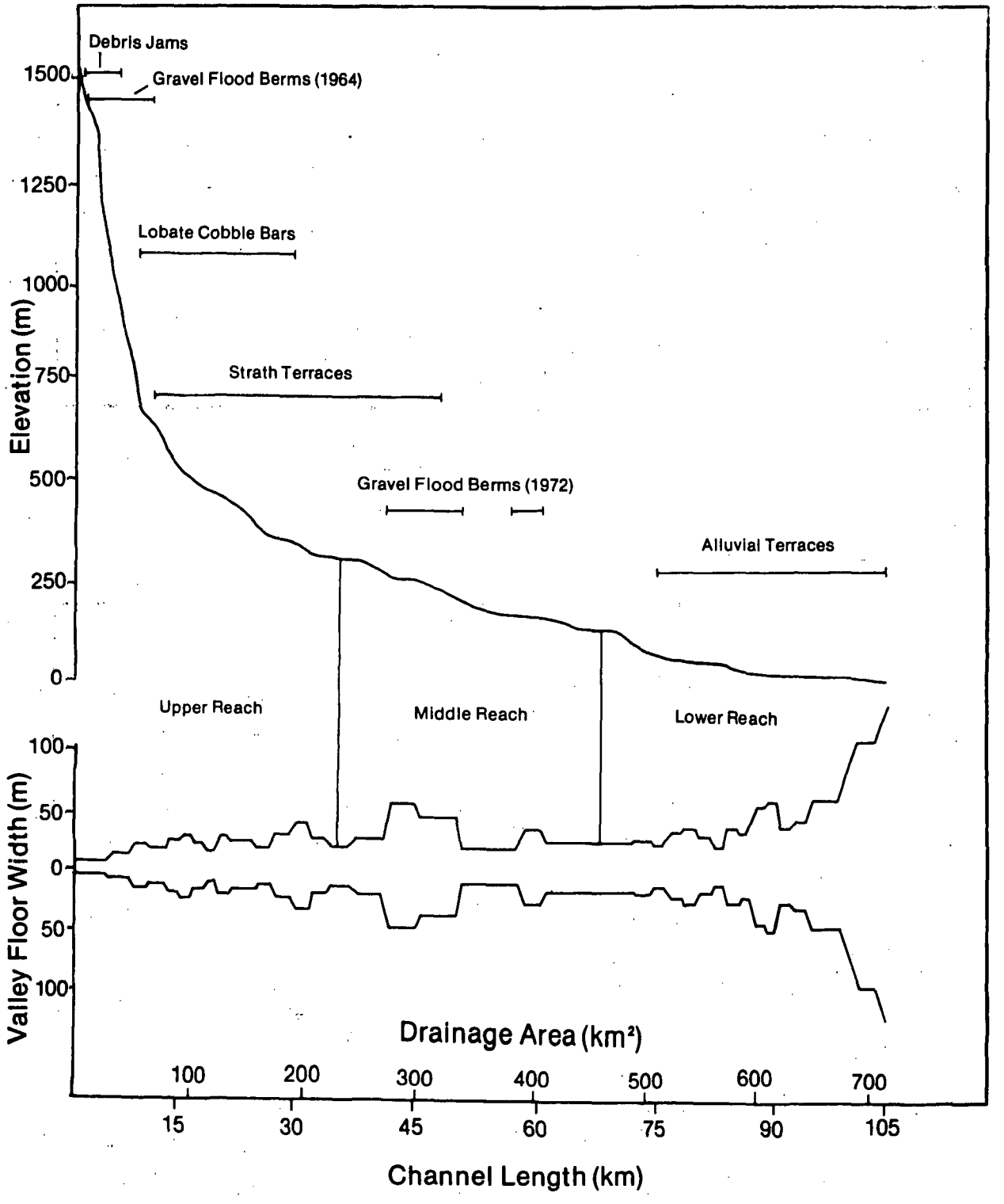

Figure 45. Longitudinal profile of Redwood Creek showing distribution of localized sediment compartments along certain reaches of the creek. Valley widths for Redwood Creek are drawn on the same horizontal scale as the profile. Figure from Madej 1984.

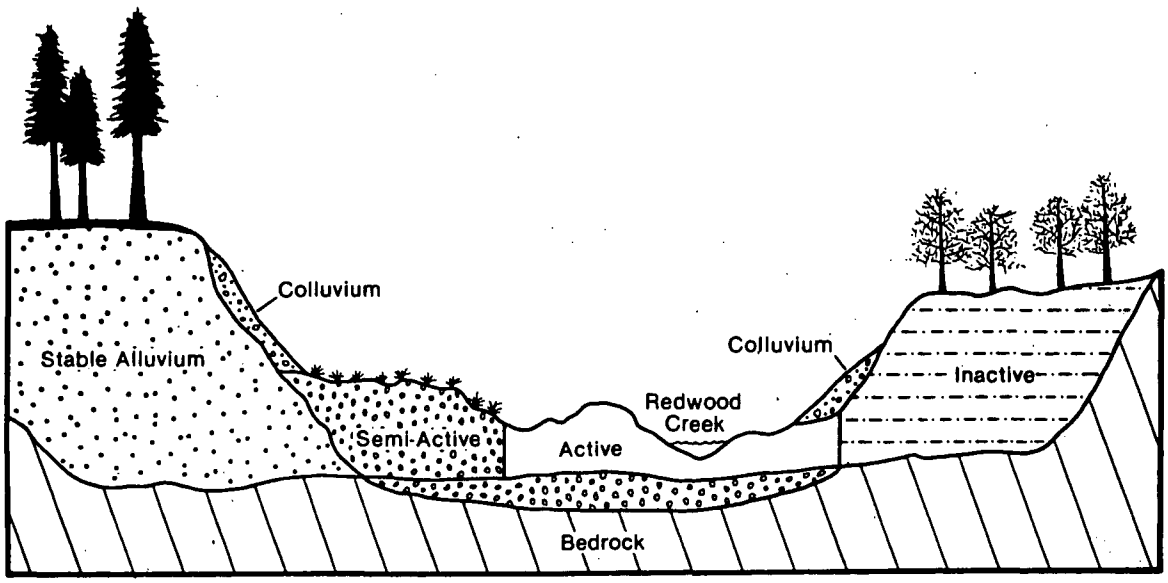

Figure 46.a. Schematic cross section of four sediment reservoirs in Redwood Creek: active (Ac), semi-active (Sa), inactive (Ia) and stable (St) sediment. Figure from Madej, 1984.

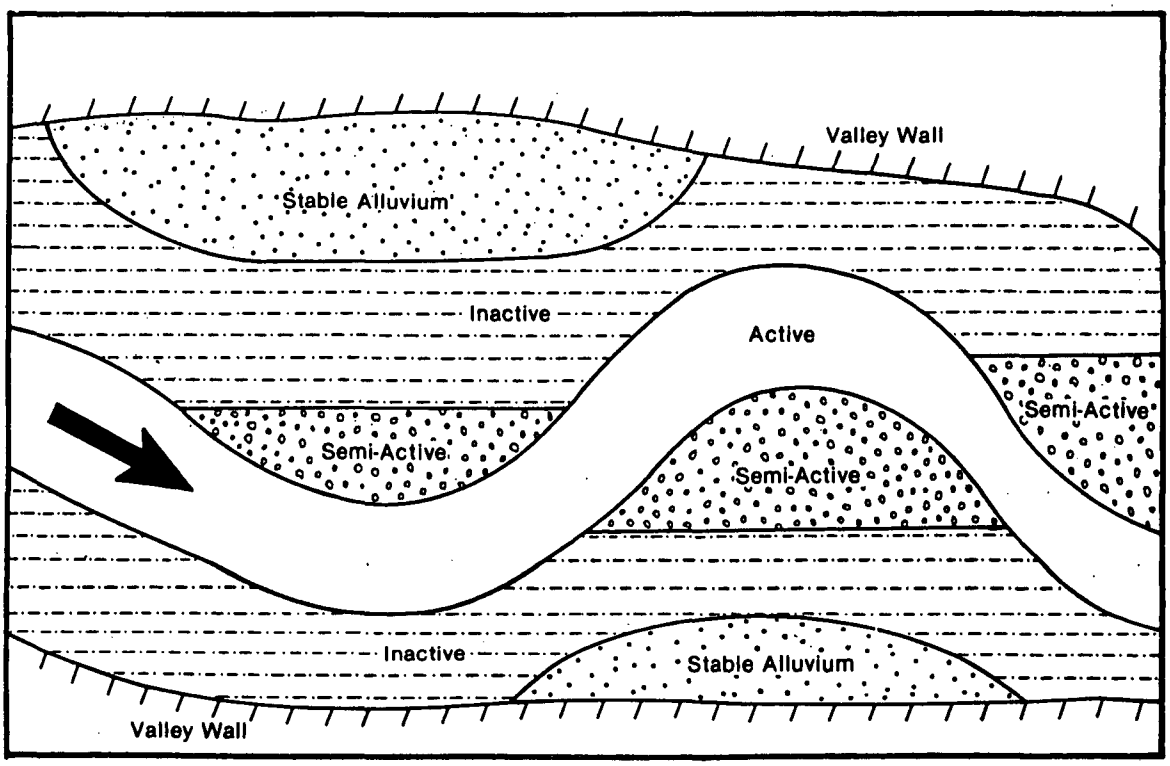

Figure 46.b. Schematic plan view of four sediment reservoirs in Redwood Creek. Figure from Madej, 1984.

scour increases downstream for equivalent discharges and depth of scour increases with increasing discharge at a given station. Sediment was not distributed uniformly downstream and maximum recent deposition occurred in areas of previous deposition. Sediment distribution is controlled more by valley width than by channel gradient, sites of sediment input, or drainage area. Fig. 47 shows the cumulative volume and spatial distribution of stored sediment in Redwood Creek for 1947, 1964, and 1980.

Erosion of bed sediment that had been deposited in the 1964 flood contributed greatly to annual bedload transport in the upper reaches of Redwood Creek for several years after the 1964 flood. Current sediment yields for Redwood Creek are 2,700 metric tons per square kilometer per year ($t/km^2/yr$) in the upper basin and 2,200 $t/km^2/yr$ at the mouth, and bedload constitutes 20% and 11% of the total load at these stations, respectively.

Residence times of active and semi-active sediment generally decrease downstream, but increase for stable sediment. Residence times range from decades for sediment in the active channel bed to thousands of years for sediment in stable floodplain deposits. Table 1 shows residence times for sediment in the four different sediment storage reservoirs for the upper, middle, and lower study reaches (located on Figures 44 and 46a). Average velocities of stored sediment are highest for active sediment, and decrease with decreasing activity levels. Recovery time for the channel in response to the 1964 flood has been slow, and total recovery will take more than a century.

We will leave stop 2 at 1:30 p.m. Return to Highway 101.

82.4 Highway 101; turn right.

83.5 Junction with Hilton Rd.; turn left on Hilton Rd. We are entering part of the previously-logged portion of Redwood National Park. All around us is relatively new vegetation, mainly hardwoods, which impair our ability to see any vistas. Our route through this part of the park is southeast along the divide between Redwood Creek drainage and Stone Lagoon drainage, and then northwest into the tributary basin of McArthur Creek and southeast into the Tom McDonald Creek basin (Fig. 37).

Slope processes active in the part of Redwood Creek underlain by schist include debris flows, block glide-earthflow complexes and soil creep. Our two stops within the park will be at debris flows, but it is important to note that much larger translational landslides do occur in the forested area of the park underlain by schist (see Sonnevil and others, this volume).

Recent rainy winters have caused extensive landsliding in the park. Sonnevil and LaHusen (personal communication) have located 40 debris flows which occurred in the winter of 1981-82 and 28 resulting from storms in the winter of 1982-83, virtually all on schist terrain. These debris flows are associated with a) steep slopes, b) topographic position below convex breaks-in-slope in headwater swales and inner gorges (see below),

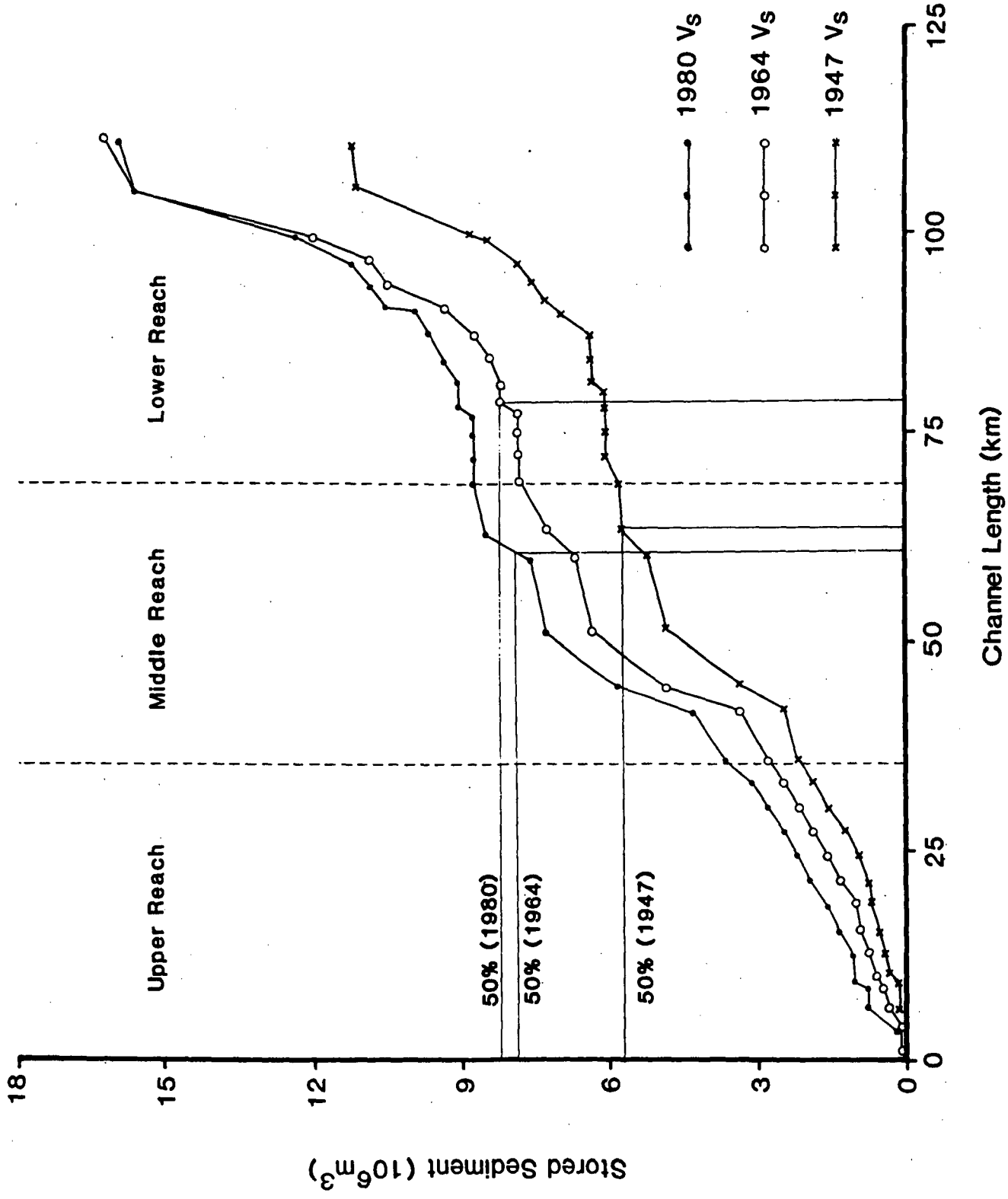

Figure 47. Cumulative volume and spatial distribution of stored sediment in Redwood Creek as of 1947, 1964 and 1980. Center of mass for each time period is indicated by the "50%" line. Note that the center of mass moved upstream after the 1964 flood, subsequently shifting 17 km downstream (as of 1980) as Redwood Creek redistributes sediment. Figure from Madej, 1984.

TABLE 1

Residence times of sediment in storage reservoirs.

Sediment Reservoirs	Residence Time Functions	Years	Velocity, V m/yr
Active	$0.09\,[X_2^{0.54} - X_1^{0.54}]$		
-upper reach (35.5 km)		26	1365
-middle reach (33.3 km)		11	3030
-lower reach (35.6 km)		9	3950
Semi-active	$0.33\,[X_2^{0.48} - X_1^{0.48}]$		
-upper reach		50	710
-middle reach		19	1750
-lower reach		15	2370
Inactive	$2.63 \times 10^{-3}\,[X_2^{1.01} - X_1^{1.01}]$		
-upper reach		104	340
-middle reach		99	335
-lower reach		106	335
Stable	$1.76 \times 10^{-9}\,[X_2^{2.55} - X_1^{2.55}]$		
-upper reach		700	50
-middle reach		3100	10
-lower reach		7200	5

c) specific soils (especially the Devilscreek soils) with a mottled subsurface horizon indicative of periodically saturated conditions, and d) the position of logging roads and skid trails (LaHusen, 1984). LaHusen (1984) postulates that compaction of soil horizons due to the placement of the road and skid trail fills may have lowered the permeability of the Devilscreek soils. Consequently, increased pore water pressures and partial saturation of the road fills caused by elevated groundwater levels may be important debris flow initiation mechanisms.

In the Van Duzen basin, we saw the prevalence of debris slides at slope positions just below the break-in-slope of the inner gorge. In lower Redwood Creek basin, shallow debris flow-type failures are also prevalent just downslope of the broad, convex divides of many Redwood Creek tributaries. Figure 48, a sketch taken from LaHusen (1984), shows both of the common hillslope positions of debris slides and debris flows in the Redwood Creek basin: inner gorge and below broad, convex divides. Our first stop this afternoon will be at a slope break just below a broad divide.

Figure 49 depicts a hillslope profile illustrating a typical debris flow initiation site. Although soil thickness and, in some instances, soil types may vary, locally all debris flow initiation sites exhibit common hydrologic and physical controls. These include a marked decrease in permeability and increase in cohesion of materials below failure surfaces. All failures examined occurred at the boundary between regolith (predominantly colluvium) and bedrock. In some locations, particularly those occurring in the upper hillslope positions, bedrock consists of hard schist. However, at many initiation sites, particularly most of those occurring within Devilscreek soils, bedrock consists of a highly sheared, dark black, quartz-mica-feldspar schist with abundant carbonaceous material.

The focus of the on-going research we will see at the next two stops is the development of models for the debris flows, with particular emphasis on determining the hydrologic characteristics of the soil and the groundwater response during storms.

86.5 Road is on a flat beveled alluvial surface between McArthur Creek and Stone Lagoon.

87.6 Road drops into McArthur Creek. Road cuts expose Redwood Creek schists.

90.1 The high bankcut on the right exposes soils of the Trailhead series (Ultisols: clayey, oxidic, isomesic Orthoxic Tropohumults). These soils have reddish (5YR to 2.5YR) clay argillic Bt horizons ranging from about 1.5 to 3 meters thick. There is 40 to 60 percent clay in the argillic horizon. Trailhead soils are found on most of the broad, rolling ridges and upper sideslopes underlain by schist in Redwood National Park. Some Trailhead profiles contain remnants of terrace sediments, including rounded clasts of Franciscan sedimentary or Klamath River (plutonic) lithology. The underlying schist bedrock is strongly weathered and reddened to a depth of several meters below the paralithic contact. Advanced soil development and deeply weathered bedrock illustrate the

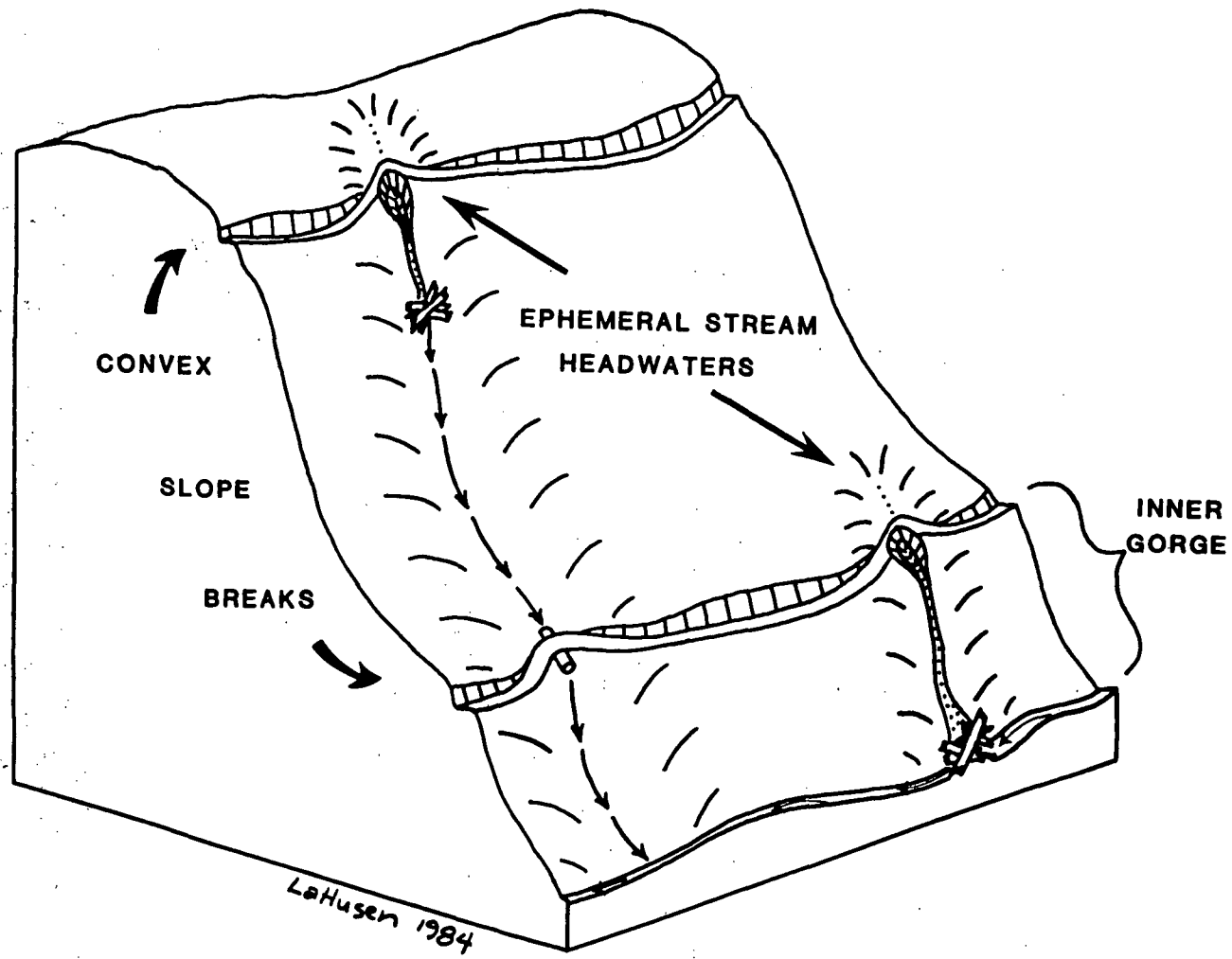

Figure 48. Diagrammatic view illustrating debris-flow-prone locations in ephemeral stream headwaters and inner gorge areas below convex slope breaks.

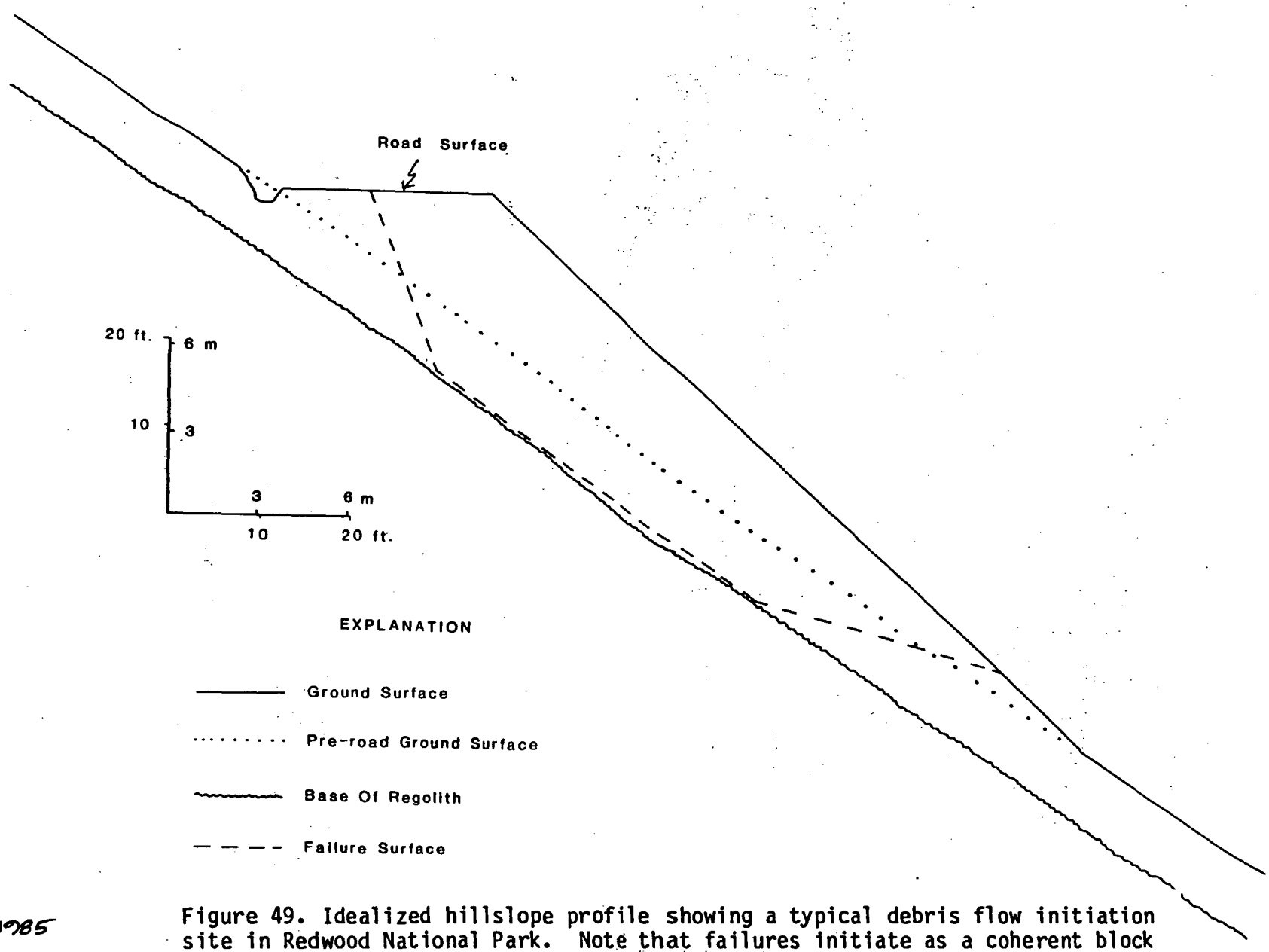

Sonnevil 1985

Figure 49. Idealized hillslope profile showing a typical debris flow initiation site in Redwood National Park. Note that failures initiate as a coherent block or "sliding wedge" and that much of the failure surface coincides with the base of the regolith.

importance of chemical dissolution in this climate on relief with comparatively low erosional activity.

90.4 Junction with L-line Road; take L-line Road to the south.

90.7 Vehicles will park in this area and we will walk 0.2 miles to Stop 3.

STOP 3 - DEBRIS FLOW ON L-LINE AND ADJACENT MONITORING SITE

This landslide failed in the winter of 1981-82, producing a debris torrent that extended into McArthur Creek and dammed the low gradient upper reach of McArthur Creek. A debris dam lake still exists in the channel (see Fig. 50.) The failure incorporated 3300 cubic yards of road fill, soil, and colluvium at the initiation site and approximately 8,000 cubic yards of regolith and organic debris were deposited in McArthur Creek. The failure occurred near the head of a swale, just below a broad, convex ridge.

Soil profiles at this stop are transitional in color and development between the strongly developed Ultisols on gentle, upper slopes and the moderately developed, brownish Inceptisols that dominate steep sideslopes. The contrast, here, between the very deep regolith in hollows and thin regolith on adjacent, convex slopes seems to be typical of upper mountain slopes in northwestern California. The well-defined soil-topographic boundary at the break-in-slope creates for us a colorful illustration of hillslope processes at work. Note the transition from reddish soils and deeply weathered bedrock at the top of the ridge to brownish soils and much fresher bedrock downslope. Note the inhomogeneity of colluvium in the hollows. It contains soil and rock in a variety of weathering states, some stratified and some mixed, all roughly traceable to a particular soil or rock source on the landscape. Use of soils as tracers could be a valuable technique for documenting geomorphic patterns and processes.

Sonnevil and LaHusen have established a monitoring network on an adjacent swale (Fig. 51) to define the groundwater movement and relate groundwater to precipitation and to slope movement processes. There were tension cracks present in this swale when the piezometers were installed. Figure 51 is a topographic map of this monitoring site showing piezometer locations and relevant morphologic features. Drilling during piezometer installations indicated that over six meters of colluvium exists within the swale upslope of the road while less than three meters are present in the swale at the base of the roadfill. This contrast indicates that this site is a colluvium-filled bedrock hollow with a bedrock lip between the road surface and the base of the roadfill.

Groundwater data at this site are being collected from an array of 24 piezometers. Piezometric stages are recorded from all piezometers on a weekly basis or after each significant rainfall event. Piezometric crests are recorded on crest staff gages (Fig. 52) and several piezometers have pressure transducers with data recorders sampling at 15 minute intervals. The data recorders and pressure transducers were designed and constructed by LaHusen. Figure 53 is a cross-section of the hillslope profile along the centerline of the swale. Piezometric data recorded in February, 1984 were used to construct this flow net for

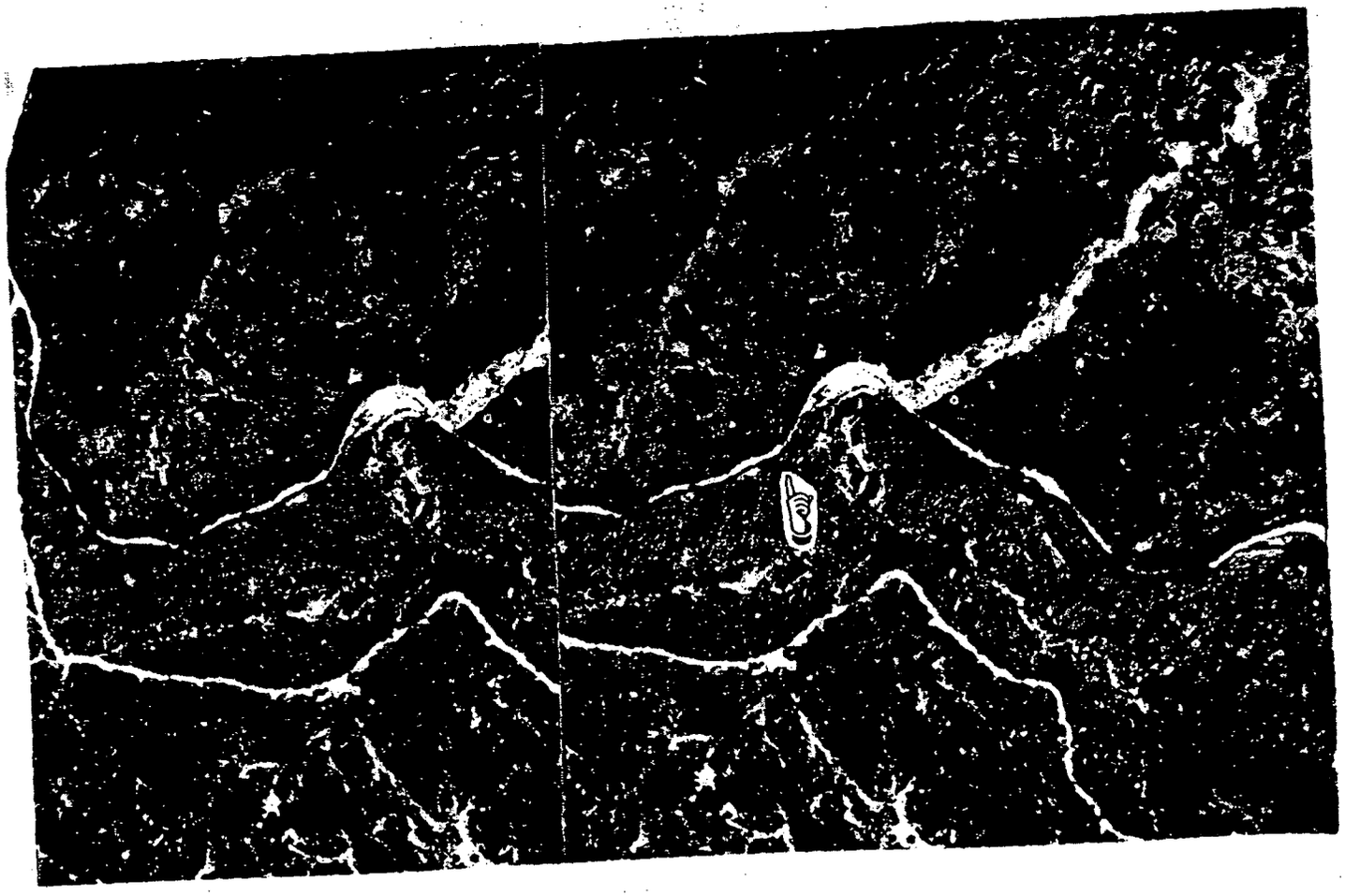

Figure 50. Stereo photo pair showing vicinity of Stop 3. Note debris torrent originating at the L-line road and resultant debris dam in McArthur Creek. Adjacent swale (marked on photo) is the groundwater monitoring site depicted in Figure 51. Debris torrent failure occurred in December 1981 and photo was taken in June 1984.

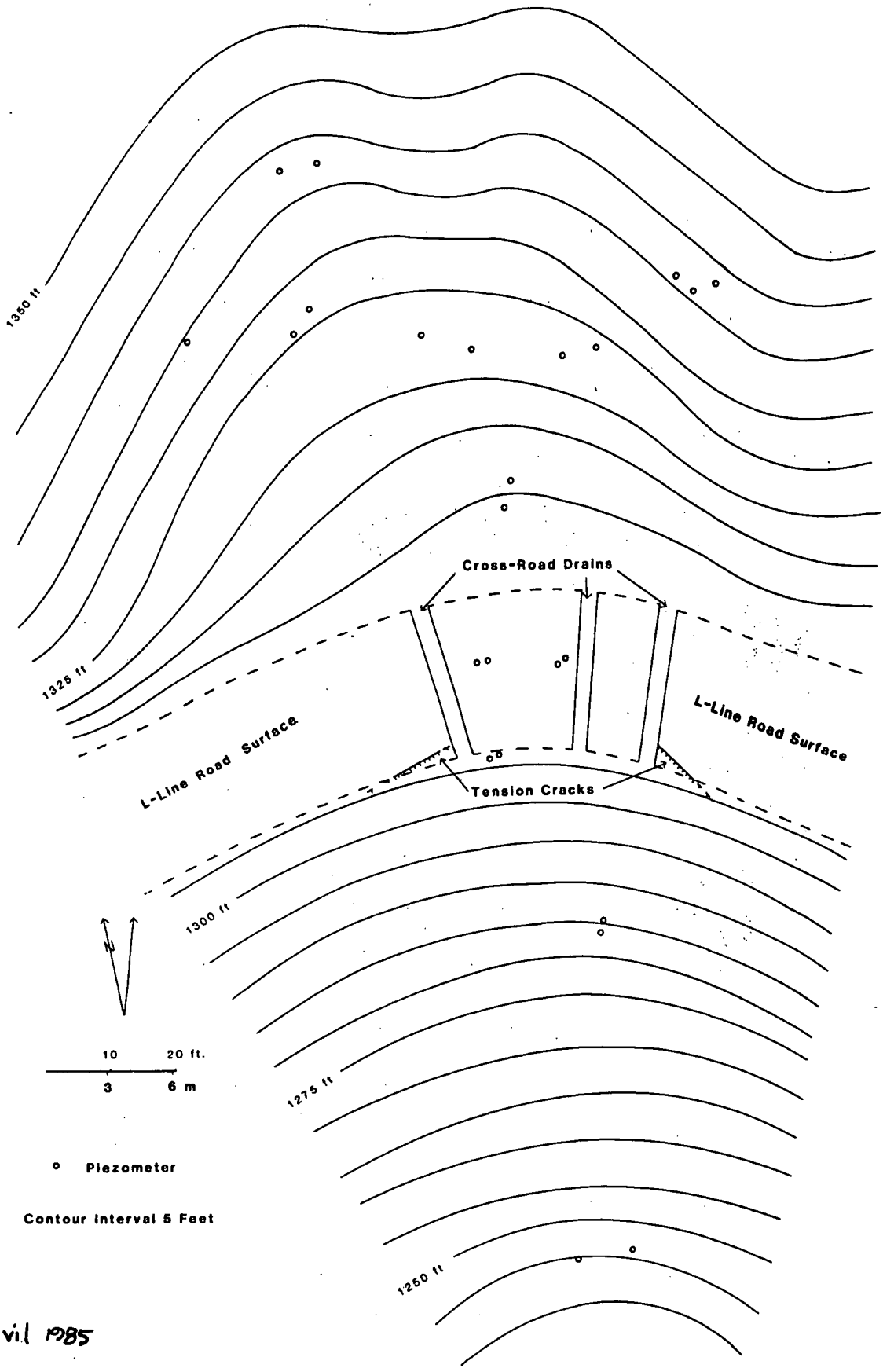

Figure 51. Topographic map showing piezometer network on and upslope of an incipient debris flow initiation site. The lower limit of roadfill coincides with the lowest piezometers. Tension cracks appeared in December 1981 and were continuous before construction of crossroad drains. Piezometers were installed in January, 1984.

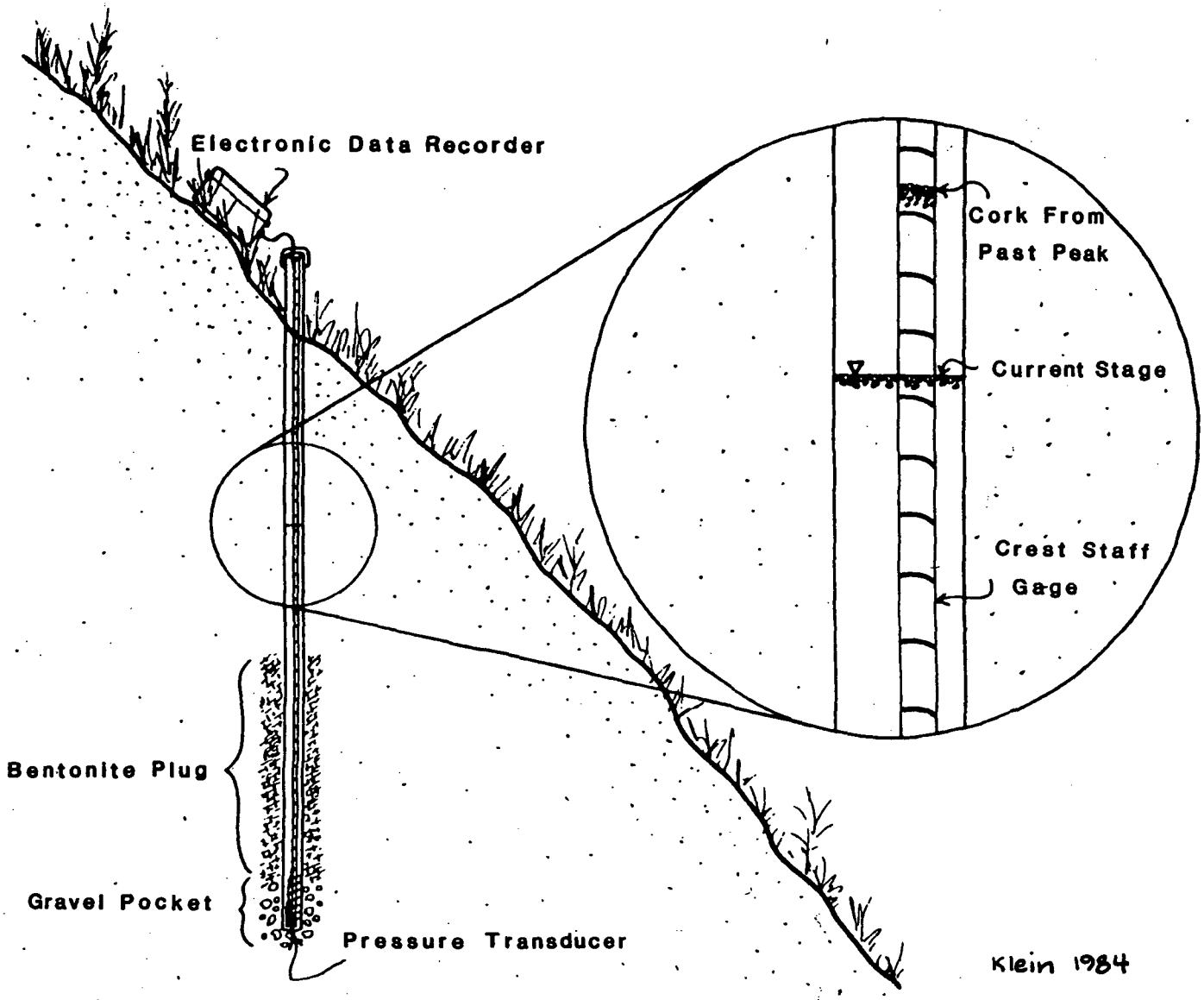

Figure 52. Diagrammatic view of piezometer installation. Piezometer casing consists of 24 mm diameter PVC pipe with the lower 45 cm slotted. Piezometers vary from 2 to 8 m in depth. Crest staff gage is a strip of PVC 12 mm wide. Past crest and current stage may be read by removing gage and noting locations of granulated cork lines. Home-made electronic instruments record piezometric stage every 15 min. on memory modules suitable for direct transfer to microcomputer system.

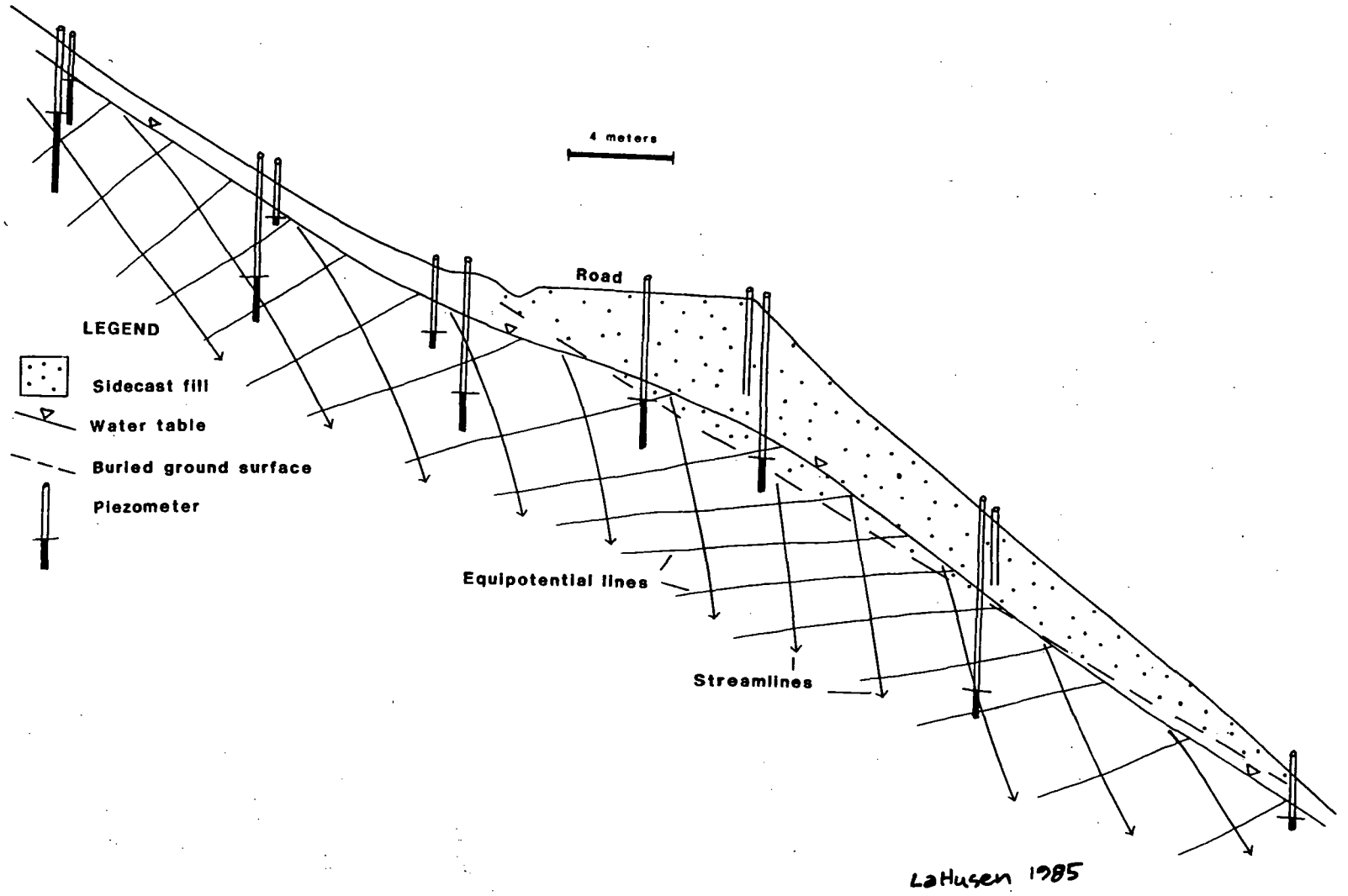

Figure 53. Hillslope cross-section along centerline of swale at Stop 3. Flow net developed from piezometric data shows elevated ground water level beneath road. Refracting streamlines are consistent with a decrease in hydraulic conductivity due to compaction of underlying soil horizons.

the saturated zone. Although only relatively minor antecedent storms (< two year return interval) occurred, evidence of groundwater perturbations is present. Note that positive pore water pressures were found within the roadfill material above the original ground surface. In addition, the downward refraction of the streamlines as they pass under the road indicate that a two- to five-fold decrease in hydraulic conductivity has occurred. More intense rainfall events would create a more pronounced "groundwater mound" eventually culminating in debris flow initiation.

Besides the hyrologic data collected at this site, four additional locations along the L-line road alignment are being monitored at a much less intensive level. Two of these locations are observable on the walk back to the vehicles. These additional monitoring sites expand the data base for a stability analysis of the L-line road fills.

Ultimately, Sonnevil and LaHusen hope to create a model of debris flow formation at this hillslope position. They will discuss some preliminary results of their modeling. One practical result of their research will be to tell rehabilitation crews how much material needs to be removed from old road fills to prevent the kind of debris flow failures obvious at this site. Removal of the entire road and landing fill prism, for instance, would have cost about $13,000 (Sonnevil, personal communication). This cost does not justify complete removal of fills, except in cases of documented imminent hazard. Twelve road fills of varying sizes are still present in swales along a mile-long reach of the the L-line road. If a way can be found to identify the fills most prone to failure and then define the minimum amount of material that needs to be removed to stabilize the slopes or greatly reduce downslope impacts, then significant savings in rehabilitation costs may result.

We plan to leave stop 3 at 3:30 p.m.

91.0 Intersection of L-line road at A-9 deck. Take A-9-9 road south.

91.9 The high, red-clay bankcut on the right exposes a Trailhead soil. This site was described and sampled by James A. DeLapp in 1960. The description and laboratory data (Sample No. 60-12-18) are published in Begg, et. al. (1984).

94.1 Turn left onto C-12 road.

94.5 Turn sharply right onto G-6-1 road. Note that the regolith generally deepens as we descend from the crest of a spur ridge onto a smooth, steep slope along the G-6 road. Smooth, steep middle and lower slope positions tend to have a continuous mantle of deep soils. Deep soils are not confined to bedrock hollows as they were at the last stop.

95.1 Exposed in the roadcut to the right are Coppercreek soils (Inceptisols: fine-loamy, mixed, isomesic Typic Humitropepts). This series and other associated Inceptisols dominate steep sideslopes in Redwood National Park. Coppercreek soils have brownish (10YR to 7.5 YR) cambic B horizons ranging from about 40 to 100 cm thick. There is 25 to 35 percent clay in the B horizon and a gradual decrease in the C horizon. Depth to bedrock

is one to three meters. The Coppercreek series is the most extensive in the park.

95.2 There are thin soils in the roadcut as we round a narrow spur and cross a well-incised stream. Thin soils are generally associated with high relief and competent bedrock. The soil profiles here were disrupted by road building. Typically, the regolith on bedrock spurs is about 50 to 100 cm deep. The Lackscreek series (loamy-skeletal, mixed, isomesic typic Humitropepts) and Ahpah series (fine-loamy, mixed, isomesic Typic Humitropepts) are the principal series. These soils have colors, horizons, and clay percentages similar to the Coppercreek series.

The valley of the next stream crossing is underlain by incompetent rock that is disintegrating and deforming downslope. The valley is broader and more irregular than the first stream valley and there are Devilscreek and Elfcreek soils on both sides of the stream. The Devilscreek series (fine-loamy, mixed, isomesic Typic Humitropepts) consists of soils similar to the Coppercreek series, except that they have a 2Cg horizon with gray matrix and brownish mottles. Water is perched during the winter rainy season and its level fluctuates within the mottled zone. The A and B horizons of Devilscreek soils probably originated by soil creep from surrounding, higher Coppercreek soils. The 2Cg horizon, which has only 8 to 20 percent clay, seems to have originated from disintegrating, but pedogenically unaltered material from within the hollow itself. The Elfcreek series (loamy-skeletal, mixed, isomesic Typic Eutropepts) have gray C horizons and grayish brown A and B horizons with 15 to 25 percent clay. They occur in locations where debris slides have removed the A and B horizon of a Devilscreek soil and also on some lobate debris flow deposits. Here, as at the last stop, contrasting soil characteristics help us keep track of slope processes.

95.3 Vehicles will park at pull-off on left. We will walk about 0.2 miles to G-6-1 debris flow.

STOP 4 - G-6-1 DEBRIS FLOW AND MONITORING SITE

This landslide failed in 1981-82 into the channel of a tributary of Tom McDonald Creek, removing some old-growth redwoods. We will look at the landslide and at the slope to the east that is being monitored by LaHusen and Sonnevil. Figure 54 is a sketch map showing the failure, groundwater monitoring sites and relevant morphologic features. The majority of soil movement and resultant debris flow at this site involved roadfill and regolith located within an intermittent stream channel. Streamflow was diverted to the north by road construction. It is evident, due to numerous tension cracks, that instability extends along the road east of the stream channel. This unstable segment of road and the adjoining hillslope is the driest of three locations being studied in detail by LaHusen who is completing a thesis at Humboldt State University on the movement of groundwater through logging road prisms constructed on Devilscreek soils.

The piezometer network at this locality consists of two parallel transects extending from upslope of the road surface to the base of the

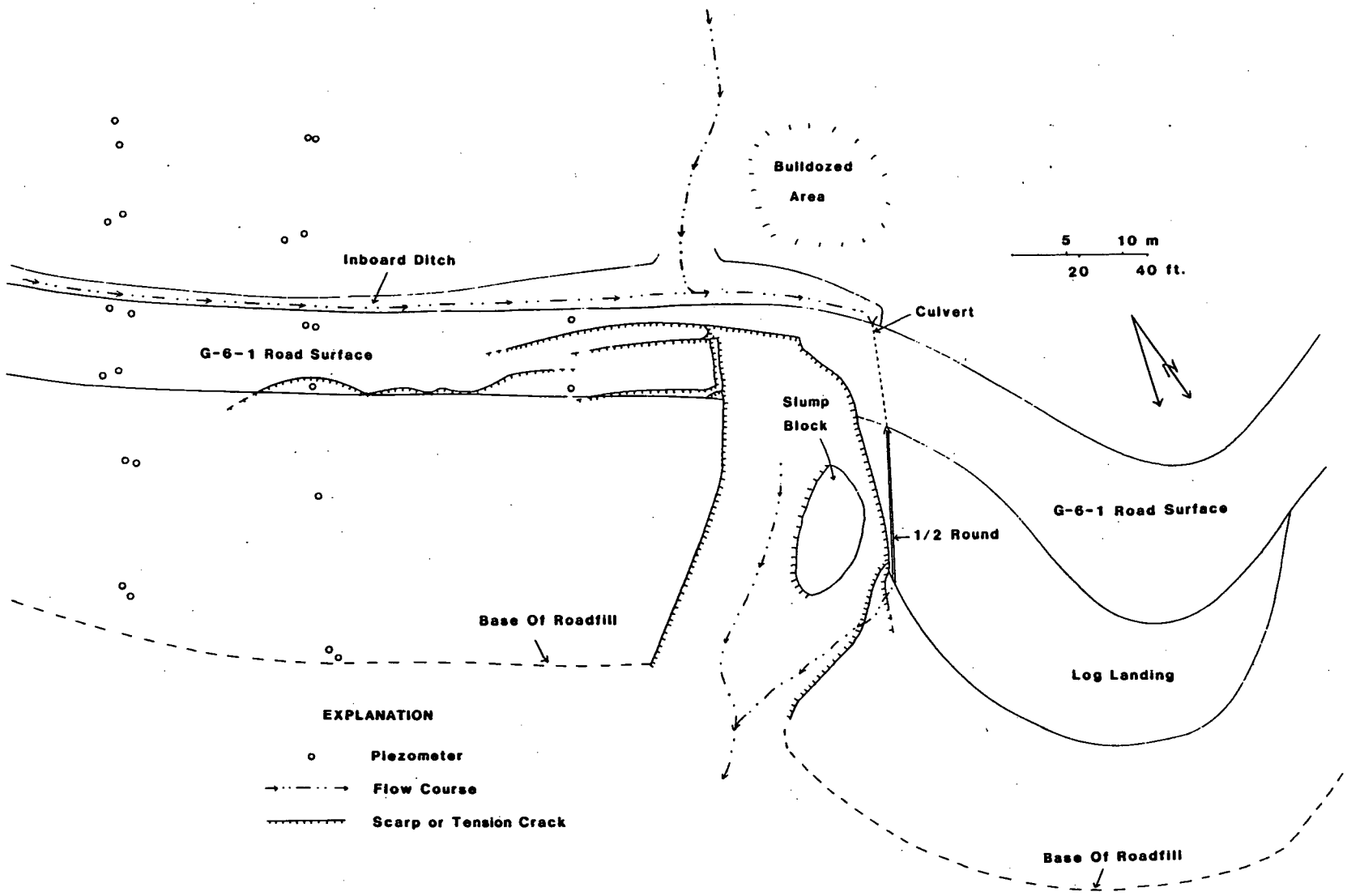

Figure 54. Map showing vicinity of Stop 4. Failure occurred in winter 1981-1982. Piezometer transects were installed in September 1983.

roadfill. Figure 55 shows a flow net generated from data collected at one of these transects in February 1984. At this site, a less obvious effect is seen compared to our last stop. Only a minor "groundwater mound" is observable beneath the road. The lesser effect is probably due to the planar hillslope where streamlines don't converge, contrasting with monitoring sites located in swales. Furthermore, for the soils along this piezometer transect, the depth from the ground surface to the top of the saturated zone is greater than in the more typical Devilscreek soils located in the next swale west of the debris flow.

Exposed along the road are examples of the wetter soils typically associated with road-related debris flows underlain by schist. Figure 56 is a sketch and description of the soil profile exposed at the piezometer transect.

We plan to leave stop 4 at 5 p.m. Those interested in a closer look at the soils in the Redwood Creek basin are encouraged to stay a little longer with Jim Popenoe, soil scientist at Redwood National Park. As many vans or buses will stay for the additional soils trip as are required. Retrace route on G-6-1, C-12, C-line and A-9-9 roads.

99.6 Mileage at deck; return to Highway 101 on Hilton Rd.

106.5 Junction Highway 101, turn south (left). We will retrace the morning's route on Highway 101 back to camp. At the south edge of Freshwater Lagoon is a prominent cliff face cut into deeply weathered Redwood Creek schists.

140.8 Junction 101 and 299. Take 299 and West End Road east, back to campground. Tonight's dinner will be a barbeque at the campground.

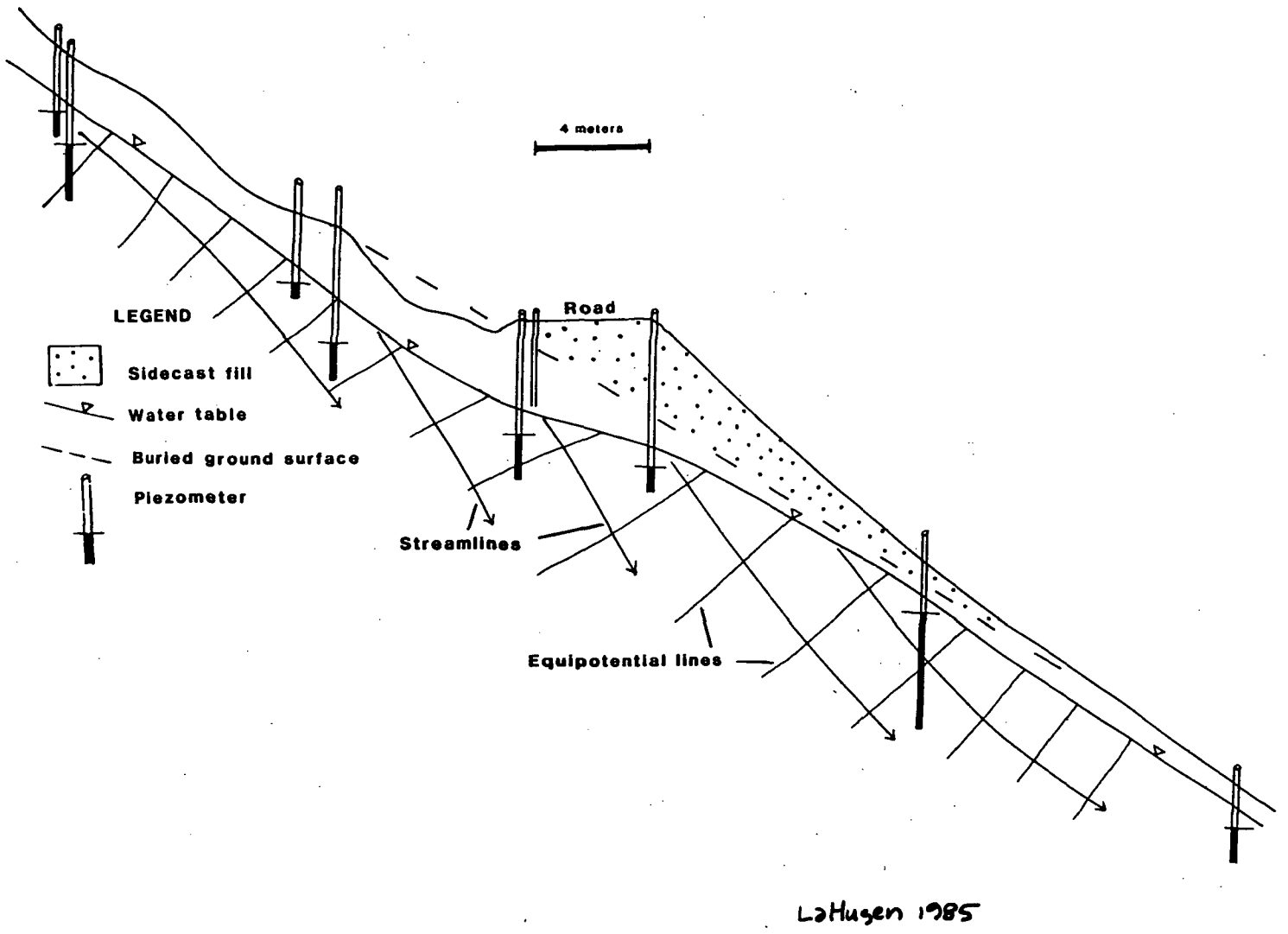

Figure 55. Hillslope cross-section of planar slope adjacent to debris flow at Stop 4. Minor "ground water mound" is evident under the road prism. A much greater elevation in ground water has been demonstrated in swales and in wetter phases of the Devilscreek soil.

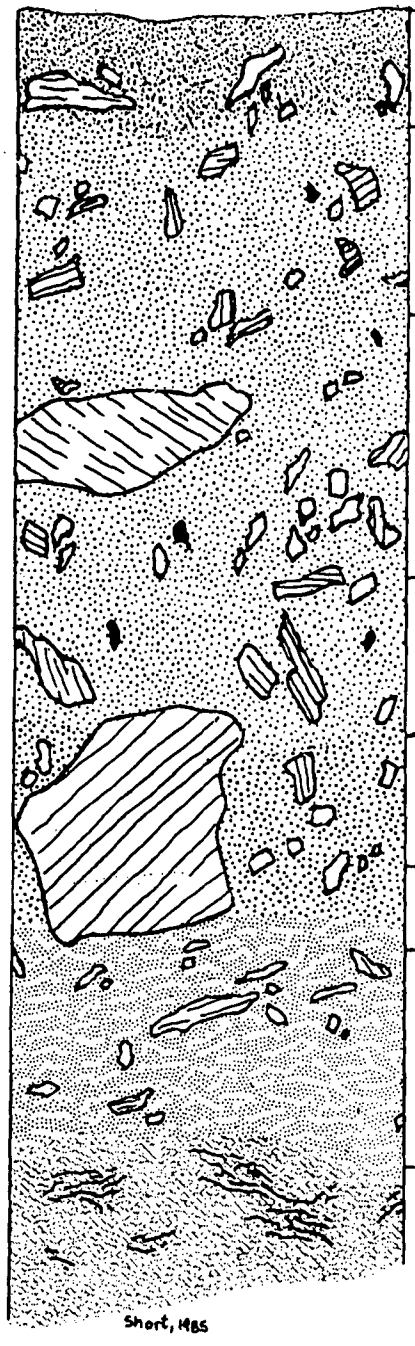

Depth (cm)		
0	A	Dark brown (10YR 3/3) very gravelly silt loam, weak fine and medium subangular blocky structure.
15	Bw1	Yellowish brown (10YR 5/6) gravelly silt loam, weak coarse & medium subangular blocky structure.
45	Bw2	Variegated strong brown, yellowish brown (7.5YR 5/6, 10YR 5/6) very cobbly silty clay loam, weak coarse subangular blocky structure.
89	Bw3	Yellowish brown (10YR 5/8) silty clay loam, weak medium subangular blocky structure.
110	BC1	Yellowish brown (10YR 5/8) very stony silty clay loam, no soil structure.
132	BC2	Yellowish brown (10YR 5/6) very stony loam, no soil structure.
145	2Cg	Variegated pale olive, gray (5Y 6/4, 5Y 5/1) gravelly loam, few brownish yellow (10YR 6/6) mottles, common brownish yellow (10YR 6/6) weathering rinds.
180	2Cr	Schist saprolite, variegated dark gray (N4/) and olive gray (5Y 5/2) few brownish yellow (10YR 6/6) weathering rinds, no mottles.

Figure 56. Sketch and description of soil profile exposed along the G-6-1 Road near piezometer transect. All colors are for moist soil.